AIP | The Journal of Chemical Physics

Analytic solution of two-density integral equations for sticky Janus dumbbells with arbitrary monomer diameters

Domenico Gazzillo, Gianmarco Munaò, and Santi Prestipino

Citation: The Journal of Chemical Physics **144**, 234504 (2016); doi: 10.1063/1.4953853
View online: http://dx.doi.org/10.1063/1.4953853
View Table of Contents: http://scitation.aip.org/content/aip/journal/jcp/144/23?ver=pdfcov
Published by the AIP Publishing

Analytic solution of two-density integral equations for sticky Janus dumbbells with arbitrary monomer diameters

Domenico Gazzillo,[1,a)] Gianmarco Munaò,[2,b)] and Santi Prestipino[2,3,c)]
[1]*Dipartimento di Scienze Molecolari e Nanosistemi, Università di Venezia, Via Torino 155, I-30172 Venezia Mestre, Italy*
[2]*Dipartimento di Scienze Matematiche ed Informatiche, di Scienze Fisiche e di Scienze della Terra, Università degli Studi di Messina, Contrada Papardo, I-98166 Messina, Italy*
[3]*CNR-IPCF, Viale F. Stagno d'Alcontres 37, I-98158 Messina, Italy*

(Received 29 February 2016; accepted 31 May 2016; published online 16 June 2016)

We study a pure fluid of heteronuclear sticky Janus dumbbells, considered to be the result of complete chemical association between unlike species in an initially equimolar mixture of hard spheres (species A) and sticky hard spheres (species B) with different diameters. The B spheres are particles whose attractive surface layer is infinitely thin. Wertheim's two-density integral equations are employed to describe the mixture of AB dumbbells together with unbound A and B monomers. After Baxter factorization, these equations are solved analytically within the associative Percus-Yevick approximation. The limit of complete association is taken at the end. The present paper extends to the more general, heteronuclear case of A and B species with size asymmetry a previous study by Wu and Chiew [J. Chem. Phys. **115**, 6641 (2001)], which was restricted to dumbbells with equal monomer diameters. Furthermore, the solution for the Baxter factor correlation functions $q_{ij}^{\alpha\beta}(r)$ is determined here in a *fully analytic* way, since we have been able to find explicit analytic expressions for all the intervening parameters. *Published by AIP Publishing.* [http://dx.doi.org/10.1063/1.4953853]

I. INTRODUCTION

Recent advances in the functionalization of colloidal particles have made available new types of "particles" with unprecedented self-assembly properties. Janus nanoparticles, made of two distinct parts bearing different functional groups, are among the most interesting new colloids.[1–3]

A simple way to model Janus colloids is to consider them as spherical particles in which one half (A) of the surface is repulsive while the other half (B) is attractive. As an immediate generalization, the simplest *Janus dumbbells* (JDs) are dimers, where a repulsive spherical monomer of chemical species A is bonded to an attractive spherical monomer of species B[4–8] (in general, these two spheres can interpenetrate each other, but in the model of this paper they are simply taken to be tangent to each other). For a more precise definition, let us consider the interaction potential between two JDs, $(AB)_1$ and $(AB)_2$, as the sum of spherically symmetric interactions between the monomers constituting the dimers, and denote A_i (B_i) the interaction site located somewhere in part A (B) of the dimer i. Then, a JD model can be characterized by assuming, for instance, that: (i) the potentials A_1–A_2, A_1–B_2, and B_1–A_2 are all repulsive, while (ii) the B_1–B_2 pair interacts through an attractive potential added to a repulsive part. The most common choice for these repulsive terms is a hard-sphere (HS) potential, while the B–B attraction may be modeled by a square-well (SW) tail. No confusion should now be possible, if such a JD molecule is synthetically indicated as a HS-SW dumbbell.

Sticky Janus dumbbells (SJDs) can finally be defined as a strongly idealized simplification of the previous HS-SW dimer model, where the B–B attraction becomes an adhesive interaction acting only when the surfaces of two B spheres are in contact. This peculiar surface contribution to the Hamiltonian is obtained following Baxter's original proposal for simple fluids:[9] one has to take the limit of a special square-well tail, in which the depth goes to infinity as the width goes to zero in such a way that the contribution to the second virial coefficient remains finite but not zero (Baxter's *sticky limit*). When the particles are monomers, this procedure generates the model of adhesive or sticky hard spheres (SHSs). Thus, our SJD molecules may also be denoted as HS-SHS dumbbells.

Nowadays, the main interest in JD lies in the fact that considerable progress in experimental synthesis does allow to fabricate this kind of colloidal molecules on a large scale, and use them as building blocks for complex supramolecular structures in biotechnology or in the fabrication of novel materials, as for instance photonics crystals. The JD, or SJD, models may also be useful to study the behavior of short surfactant molecules, which contain both a hydrophilic and a hydrophobic part.

The Janus dimers AB are, however, a particular case in the large class of *heteronuclear* colloidal dumbbells (of course, homonuclear dimers require that the species B is identical to A with respect to all properties, i.e., shape, size, and interactions, while heteronuclear dimers include even the case of monomers with identical HS

[a)]Author to whom correspondence should be addressed. Electronic mail: gazzillo@unive.it
[b)]Email: gmunao@unime.it
[c)]Email: sprestipino@unime.it

diameters but different attractive interactions). Over the last decades several investigations have been performed on homonuclear and heteronuclear colloidal dumbbells by using both experimental and theoretical approaches (see, for instance, the works cited in Ref. 4). In particular, one of us (Munaò) participated in studies[4–7] involving Monte Carlo (MC) simulations as well as the *fully numerical* solution of molecular integral equations corresponding to the so-called Reference Interaction Site Model (RISM) theory.[10]

In principle, we can imagine the assembly of a colloidal dumbbell fluid starting from an equimolar mixture of A and B monomers (we assume that only monomer reagents are initially present), which can associate together according to the reaction $A + B \rightleftarrows AB$. In general, at equilibrium the system contains both monomers and dimers. However, the equilibrium amount of dimers depends on the strength $\mathcal{B}$ of the attraction between A and B pairs. If the A–B attraction is much stronger than other possible B–B or A–A attractive interactions (as occurs when the dimerization is due to the formation of a true covalent bond), then one can, in practice, take the limit $\mathcal{B} \to \infty$ in any model representing the physical system. This extreme simplification implies that all monomers vanish and the mixture then reduces to a pure fluid containing only dimers (*complete association* limit). Our theoretical study follows exactly such a conceptual route (starting from a mixture of A, B, and AB particles, and taking the above-mentioned infinite limit at the end), trying to derive the properties of a JD pure fluid analytically, as far as possible.

To this aim, we will exploit the multidensity Ornstein-Zernike (MdOZ) integral equation theory, proposed by Wertheim for associating or chemically reactive fluids with highly directional and saturable forces.[11–15] Wertheim first developed the formalism for a single off-center attraction site,[11,12] and then for multiple off-center SW bonding sites embedded in the hard-core region.[13,14] Kalyuzhnyi and Stell[16] reformulated the theory in order to treat fluids with spherically symmetric associative interactions. The effects of steric saturations are introduced explicitly into the theory via an appropriate resummation of diagrams.

The MdOZ approach is called "multi-density," since it includes additional density parameters required to describe the possibility of different bonding states for the particles. When the associating monomers only possess a single chemical-bonding site, and the saturation of the A–B covalent bonding—due to steric effects—allows only *dimerization*, two densities for each species are necessary and sufficient to describe the mixture of monomers and dimers. Two-density, 2dOZ integral equations have been successfully employed and analytically solved for several models of associating fluids where chemical bonding generates dimers. On the other hand, for particles with two or more association sites, which can *polymerize* and form chains, rings or more complex n-mers, the MdOZ equations become more difficult to solve, since the number of required densities increases (for two association sites, with a single bonding condition, there are four densities *for each species*, leading to 4dOZ equations).

For example, analytic solutions of the 2dOZ equations, supplemented by adequate approximate closures, have been found for dimerizing fluids of: hard spheres (generating both homonuclear[15] and heteronuclear HS-HS dumbbells[17]), penetrable spheres,[18] adhesive hard spheres (producing homonuclear SHS-SHS dumbbells, with equal diameters and equal stickiness strengths,[19] or heteronuclear SHS-SHS dumbbells, with equal diameters and different stickiness strengths[20]), Yukawa particles,[21] charged hard spheres.[22–27] Analytic 4dOZ solutions are available for some models of polymer chains: for instance, freely jointed tangent HS chains (of any length, but without branches),[28] mixtures of homonuclear HS chains,[29] homonuclear SHS chains,[30] diblock polymer chains consisting of a linear HS chain linked to a linear SHS chain (both of arbitrary length),[31] polyelectrolyte ionic chains,[32,33] and multiarm star polymers.[34]

With regard to SJD, we are aware of only one work by Wu and Chiew,[37] who analytically solved 2dOZ integral equations for a dimerizing HS-SHS mixture with equal diameters $\sigma_A = \sigma_B$ and where A–B and B–B pairs interact through HS potentials, while an adhesive surface interaction acts between A–A pairs. The resulting solution depends on three parameters, λ_{00}, $\widetilde{\lambda}_{10}$, and $\widetilde{\lambda}_{11}$, which are functions of the thermodynamic state. The values of λ_{00} and $\widetilde{\lambda}_{10}$ were found by solving *numerically* an algebraic quartic equation for each parameter. Only one of the four roots is physically acceptable, and was determined by verifying that it satisfies the correct zero-density limit (see below).

The present work has mainly been suggested from the very recent MC numerical study by Munaò *et al.*[7] on heteronuclear JD fluids (HS-SW dimers with $\sigma_A \neq \sigma_B$). Our aim is twofold: (i) to extend Wu and Chiew's work, by solving analytically 2dOZ equations for HS-SHS dumbbells with arbitrarily different diameters, within the multidensity generalization of the Percus-Yevick (PY) closure; (ii) to make the solution fully analytic, in the sense that we will provide closed-form expressions for all the required parameters, which are related to the values of the cavity correlation functions at contact.

The paper is organized as follows. In Section II, after briefly restating the theory of two-density integral equations, we define the model of sticky Janus dumbbell with arbitrary monomer diameters and present the analytic solution—in terms of Baxter auxiliary functions within the associative Percus-Yevick approximation—for a mixture of associating monomers and dimers in chemical equilibrium. The complete association limit is taken in Section III, which refers to a pure fluid of SJD. Section IV discusses how we have been able to find fully analytic expressions for the $\widetilde{\lambda}_{ij}$ basic parameters. Then, in Section V we report some numerical data for the $\widetilde{\lambda}_{ij}$ as well as some structural information which can rapidly be extracted from our analytic formulas. These latter qualitative considerations should only be regarded as an anticipation to our complete study of structural and thermodynamic SJD properties deferred to a forthcoming paper. Finally, conclusive remarks are given in Section VI, while some more technical notes have been reported in the Appendices.

II. THEORY

A. Two-density integral equations: Wertheim's and Baxter's forms

In order to get an improved integral equation theory for fluids of associating molecules, Wertheim[11–14] started from the fugacity expansion for the logarithm of the grand-canonical partition function, and reorganized the graphs of its diagrammatic representation into n-mer subsets, thus more easily showing the cancellation of some graphs due to steric incompatibility. After a topological reduction, he obtained—for particles with a single saturable bonding site—an expansion of the correlation functions in terms of two densities for each chemical species α: the total density ρ_α, and the density ρ_0^α of the monomers of species α which are still free, i.e., unbound, in the actual mixture of monomer and dimers (according to Wertheim's new point of view, the set of all particles of *each species* must be regarded as *a mixture* of unbound and bound monomers, with an *own* "internal" molar fraction: in fact, $x_0^\alpha = \rho_0^\alpha/\rho_\alpha$ is the molar fraction of the unbound monomers "inside" the species α). For a homogeneous fluid, the two-density expansion of the total correlation functions $h_{\alpha\beta}(r)$ in terms of partial total correlation functions $h_{ij}^{\alpha\beta}(r)$ reads as[11–14,16,18]

$$\rho_\alpha h_{\alpha\beta}(r)\rho_\beta = \rho_\alpha h_{00}^{\alpha\beta}(r)\rho_\beta + \rho_0^\alpha h_{10}^{\alpha\beta}(r)\rho_\beta + \rho_\alpha h_{01}^{\alpha\beta}(r)\rho_0^\beta + \rho_0^\alpha h_{11}^{\alpha\beta}(r)\rho_0^\beta, \quad (1)$$

or

$$h_{\alpha\beta}(r) = h_{00}^{\alpha\beta}(r) + x_0^\alpha\, h_{10}^{\alpha\beta}(r) + x_0^\beta\, h_{01}^{\alpha\beta}(r) + x_0^\alpha x_0^\beta\, h_{11}^{\alpha\beta}(r) \quad (2)$$

(r denotes the distance between the centers of two monomers of species α and β). A similar two-density expansion can be given for the direct correlation functions (DCFs) $c_{\alpha\beta}(r)$.

In the $h_{ij}^{\alpha\beta}(r)$'s (sometimes also written as $h_{\alpha\beta}^{ij}(r)$[25,26,32,33]) the greek indices refer to the chemical species, while the latin ones i, j specify the degree of association, or particle coordination number, i.e., the two possible bonding states of a particle: unbound (index 0) for free monomers, and bound (index 1) for monomers involved in dimers. More precisely, the subscripts in $h_{ij}^{\alpha\beta}(r)$ indicate the number of f_b chemical bonds incident on each of the root points in the diagrams for $h_{\alpha\beta}(r)$[18] (f_b is related to the Mayer function corresponding to the covalent association potential). For example, $h_{01}^{\alpha\beta}$ denotes the sum of all diagrams with no f_b bonds incident on the first root point of species α, but one f_b bond incident on the second root point of species β (see Fig. 1 of Ref. 18).

Similar two-density expansions can be written also for other correlation functions, such as the radial distribution functions (RDFs) $g_{\alpha\beta}(r) = 1 + h_{\alpha\beta}(r)$ and the DCF's $c_{\alpha\beta}(r)$. One immediately finds that

$$g_{ij}^{\alpha\beta}(r) = \delta_{i0}\delta_{j0} + h_{ij}^{\alpha\beta}(r). \quad (3)$$

Let us introduce, for the total and direct correlation functions, the *matrices of matrices* $\mathbb{H}(r)$ and $\mathbb{C}(r)$, respectively. This means that $\mathbb{H}(r)$ and $\mathbb{C}(r)$ are matrices, whose elements are in turn 2×2-matrices, i.e.,

$$[\mathbb{H}(r)]_{\alpha\beta} = \boldsymbol{h}_{\alpha\beta}(r), \qquad [\mathbb{C}(r)]_{\alpha\beta} = \boldsymbol{c}_{\alpha\beta}(r). \quad (4)$$

The elements of $\boldsymbol{h}_{\alpha\beta}(r)$ are given by

$$\boldsymbol{h}_{\alpha\beta}(r) = \begin{bmatrix} h_{00}^{\alpha\beta}(r) & h_{01}^{\alpha\beta}(r) \\ h_{10}^{\alpha\beta}(r) & h_{11}^{\alpha\beta}(r) \end{bmatrix}, \quad (5)$$

and those of $\boldsymbol{c}_{\alpha\beta}(r)$ are similar. For the two-density case, the density matrix is defined as

$$\boldsymbol{\rho} = \begin{bmatrix} \boldsymbol{\rho}_A & \mathbf{0} \\ \mathbf{0} & \boldsymbol{\rho}_B \end{bmatrix}, \quad (6)$$

where the elements $\mathbf{0}$ are 2×2 null matrices and

$$\boldsymbol{\rho}_\alpha = \begin{bmatrix} \rho_\alpha & \rho_0^\alpha \\ \rho_0^\alpha & 0 \end{bmatrix} = \rho_\alpha \begin{bmatrix} 1 & x_0^\alpha \\ x_0^\alpha & 0 \end{bmatrix} \qquad (\alpha = A, B). \quad (7)$$

In general, Wertheim's orientation-averaged multidensity integral equations can be written in Ornstein-Zernike-like form as

$$\boldsymbol{h}_{\alpha\beta}(r) = \boldsymbol{c}_{\alpha\beta}(r) + \sum_\gamma \int d\boldsymbol{r}'\, \boldsymbol{c}_{\alpha\gamma}(r')\boldsymbol{\rho}_\gamma \boldsymbol{h}_{\gamma\beta}(|\boldsymbol{r} - \boldsymbol{r}'|). \quad (8)$$

Here, the $\boldsymbol{\rho}_\gamma$ matrices are essential, since the condition $(\boldsymbol{\rho}_\gamma)_{11} = 0$ eliminates all diagrams which violate the saturation condition of at most one f_b chemical bond per particle in dimerizing fluids.

Furthermore, the equilibrium density ρ_0^α of free monomers of species α can be determined in terms of ρ_α via the self-consistent relation[15]

$$\rho_\alpha = \rho_0^\alpha + \rho_1^\alpha = \rho_0^\alpha + \rho_0^\alpha \sum_\gamma \rho_0^\gamma \int d\boldsymbol{r}\, f_b^{\alpha\gamma}(r) g_{00}^{\alpha\gamma}(r), \quad (9)$$

where $g_{00}^{\alpha\gamma}(r) = 1 + h_{00}^{\alpha\gamma}(r)$ and ρ_1^α is the density of α-monomers bound in A–B dimers. This equation is equivalent to the law of mass action for chemical equilibrium, and shows how ρ_0^α and ρ_1^α depend on the features of the association interactions, expressed through the Mayer functions f_b corresponding to the chemical bonds.

By working in k-space with the Fourier transforms $\widehat{\mathbb{H}}(k)$ and $\widehat{\mathbb{C}}(k)$, Eq. (8) can be even more compactly reshuffled as

$$\widehat{\mathbb{H}}(k) = \widehat{\mathbb{C}}(k) + \widehat{\mathbb{C}}(k)\boldsymbol{\rho}\widehat{\mathbb{H}}(k), \quad (10)$$

or, in a form more adequate for factorization,

$$\left[\boldsymbol{\rho}^{-1} - \widehat{\mathbb{C}}(k)\right]\left[\mathbb{I} + \boldsymbol{\rho}\widehat{\mathbb{H}}(k)\right] = \boldsymbol{\rho}^{-1}, \quad (11)$$

$\mathbb{I}$ being the unit matrix.

By employing the Baxter-Wertheim factorization and introducing the auxiliary factor correlation functions, given here by the matrices $\boldsymbol{q}_{\alpha\beta}(r)$ with elements $q_{ij}^{\alpha\beta}(r)$, Eq. (8) are usually re-expressed in the more convenient Baxter system[22,35,36]

$$\begin{cases} r\boldsymbol{h}_{\alpha\beta}(|r|) = -\boldsymbol{q}'_{\alpha\beta}(r) + 2\pi \sum_\gamma \int_{L_{\alpha\gamma}}^{\infty} dz\, \boldsymbol{q}_{\alpha\gamma}(z)\, \boldsymbol{\rho}_\gamma \boldsymbol{h}_{\gamma\beta}(|r-z|)\,(r-z)\,, \\ r\boldsymbol{c}_{\alpha\beta}(|r|) = -\boldsymbol{q}'_{\alpha\beta}(r) + 2\pi \sum_\gamma \dfrac{\partial}{\partial r} \int_{L_{\gamma\alpha}}^{\infty} dz\, \boldsymbol{q}_{\gamma\alpha}(z)\, \boldsymbol{\rho}_\gamma \boldsymbol{q}_{\gamma\beta}(r+z), \end{cases} \tag{12}$$

for $r > L_{\alpha\beta}$, where $L_{\alpha\beta} = (\sigma_\alpha - \sigma_\beta)/2$ (σ_α being the HS diameter of species α). The prime denotes differentiation with respect to r.

Finally, it is worth stressing that the Baxter form of the MdOZ integral equations is tantamount to finding the analytic expressions of the $q_{ij}^{\alpha\beta}(r)$'s, from which all structural and thermodynamic properties of the fluid can be calculated, analytically or numerically. According to this point of view, the solution at which we will arrive is *fully analytic*, since it determines these auxiliary Baxter functions in a complete way, including the explicit expressions of all their parameters.

B. SJD potential model and closure

Let us imagine to start from a fluid containing only reagents, i.e., a binary equimolar mixture of monomers A and B, with $\rho_A = \rho_B$ and arbitrary HS diameters σ_A and σ_B with the additive sum rule $\sigma_{\alpha\beta} = (\sigma_\alpha + \sigma_\beta)/2$. At equilibrium, one has a ternary mixture with $\rho_0^A = \rho_0^B$, including the dimers formed by the association reaction (their density is $\rho_{\rm dim} = \rho_1^A = \rho_1^B$).

We assume that the A–A interaction u_{AA} is a HS one, while the B–B pairs interact through a sticky surface potential (in our paper the roles of A and B are interchanged with respect to Ref. 37). The A–B covalent bonding can still be represented by a SHS potential (here named SHS*), but is however rather different with respect to the B–B attraction.[37] In fact, apart from its much stronger strength, $u_{AB}^{\rm SHS^*}$ must generate a "saturable" chemical bond (no more than one B-particle can be bonded to one A-particle), where $u_{BB}^{\rm SHS}$ refers to a "non-saturable" physical (dispersion) attraction, since more than one B-particle can adhere to another B-particle. The above-mentioned saturation constraint cannot be expressed by a spherically symmetric SHS* potential, but the anisotropic, directional nature of the covalent bond is nevertheless introduced into the Wertheim-OZ theory through the steric incompatibilities.

After recalling that the Mayer functions for HS potentials are

$$f_{\alpha\beta}^{\rm HS}(r) = \exp\left[-\beta u_{\alpha\beta}^{\rm HS}(r)\right] - 1 = \begin{cases} -1, & 0 \le r < \sigma_{\alpha\beta} \\ 0, & r > \sigma_{\alpha\beta} \end{cases} \tag{13}$$

(with $\beta = (k_{\rm B}T)^{-1}$, where $k_{\rm B}$ is the Boltzmann's constant and T the absolute temperature), our model for *sticky Janus dumbbells* can be defined by choosing

$$\begin{cases} f_{AA}(r) = f_{AA}^{\rm HS}(r), \\ f_{BB}(r) = f_{BB}^{\rm SHS}(r) = f_{BB}^{\rm HS}(r) + t\,\sigma_B \delta(r-\sigma_B), \\ f_{AB}(r) = f_{AB}^{\rm SHS^*}(r) = f_{AB}^{\rm HS}(r) + k_{\rm chem}\,\sigma_{AB}\delta(r-\sigma_{AB}), \end{cases} \tag{14}$$

and $f_{BA}(r) = f_{AB}(r)$. Here, the Dirac delta function δ in f_{BB} and f_{AB} ensures that both the physical adhesion and the chemical association forces act only at the corresponding contact surfaces. The factors t and $k_{\rm chem}$ express the relevant strengths. More precisely,

$$t = \frac{1}{12\tau} \tag{15}$$

is our measure of the B–B adhesion strength, so that $t \to 0$ corresponds to the limiting case of pure HS potential. On the other hand, τ ($\equiv \tau_{BB}$ here) denotes the dimensionless parameter introduced by Baxter into his original definition of the SHS potential.[9] The value of τ is also an (not fully defined) increasing function of the temperature: it must be zero at the absolute zero, and if $T \to \infty$, then τ must diverge too. Consequently, low τ (high t) values correspond to low temperatures and/or strong B–B adhesive forces. The strength of chemical bond, $k_{\rm chem}$, is independent of t. Later, complete association of monomers into dimers will be obtained by taking the limit $k_{\rm chem} \to \infty$.

The presence of hard cores in all the considered interactions implies that any solution to the MdOZ equations must satisfy the exact HS conditions

$$g_{ij}^{\alpha\beta}(r) = 0, \quad \text{or} \quad h_{ij}^{\alpha\beta}(r) = -\delta_{i0}\delta_{j0}, \quad \text{for } 0 < r < \sigma_{\alpha\beta}, \tag{16}$$

where δ_{ij} is the Kronecker delta. As for the closure, we adopt the following multidensity generalization of the Percus-Yevick (PY) approximation to the DCF's:

$$\begin{cases} c_{ij}^{AA}(r) = 0, & r \ge \sigma_A, \\ c_{ij}^{BB}(r) = \lambda_{ij}\,\sigma_B \delta(r-\sigma_B), & r \ge \sigma_B, \\ c_{ij}^{AB}(r) = \mathcal{B}_{ij}\,\sigma_{AB}\delta(r-\sigma_{AB}), & r \ge \sigma_{AB}, \end{cases} \tag{17}$$

and $c_{ij}^{BA}(r) = c_{ij}^{AB}(r)$, with

$$\begin{cases} \lambda_{ij} = t\; y_{ij}^{BB}(\sigma_B), \\ \mathcal{B}_{ij} = \delta_{i1}\delta_{j1}\,\mathcal{B}, \quad \text{where} \quad \mathcal{B} = k_{\rm chem}\; y_{00}^{AB}(\sigma_{AB}). \end{cases} \tag{18}$$

Here, $y_{ij}^{\alpha\beta}(\sigma_{\alpha\beta})$ is the contact value of the ij-component of the cavity correlation function $y_{\alpha\beta}(r)$, which is defined through the relationship

$$g_{\alpha\beta}(r) = y_{\alpha\beta}(r)\exp[-\beta u_{\alpha\beta}(r)], \tag{19}$$

with $u_{\alpha\beta}(r)$ being the α–β interaction potential. The quantities λ_{ij}'s refer to the SHS (dispersion) interaction between B–B pairs, and are yet unknown parameters to be determined later (other authors[19,37] define $\lambda_{ij} = y_{ij}^{BB}(\sigma_B)/\tau$, without including $\frac{1}{12}$). On the other hand, the $\mathcal{B}_{ij}$'s are related to the A–B chemical association, but only $\mathcal{B}_{11} = \mathcal{B}$ differs from zero.

In the literature, the closure (17) was sometimes referred to as the "associative Percus-Yevick" (APY) approximation.[17]

In particular, the expressions of $c_{ij}^{AA}(r)$ and $c_{ij}^{BB}(r)$ simply reflect the usual PY closure, while the expression of c_{ij}^{AB} for associating particles is known as "polymer PY" (PPY) approximation.[37] The three DCF approximations of the APY closure can be summarized into a single compact expression by writing

$$c_{ij}^{\alpha\beta}(r) = K_{ij}^{\alpha\beta}\,\sigma_{\alpha\beta}\delta(r-\sigma_{\alpha\beta}),\ r \geq \sigma_{\alpha\beta}, \tag{20}$$

with

$$\begin{cases} K_{ij}^{AA} = 0, \\ K_{ij}^{BB} = \lambda_{ij}, \\ K_{ij}^{AB} = K_{ij}^{BA} = \mathcal{B}_{ij}. \end{cases} \tag{21}$$

Since both c_{ij}^{BB} and c_{ij}^{AB} include a Dirac δ-term "at" contact, these DCF's can be expressed as the sum of a "regular" part and a "singular" δ-contribution. The same singular terms must appear in h_{ij}^{BB} and h_{ij}^{AB}, so that it is convenient to write

$$\begin{aligned} c_{ij}^{\alpha\beta}(r) &= c_{ij}^{\alpha\beta,\mathrm{reg}}(r) + K_{ij}^{\alpha\beta}\,\sigma_{\alpha\beta}\delta(r-\sigma_{\alpha\beta}), \\ h_{ij}^{\alpha\beta}(r) &= h_{ij}^{\alpha\beta,\mathrm{reg}}(r) + K_{ij}^{\alpha\beta}\,\sigma_{\alpha\beta}\delta(r-\sigma_{\alpha\beta}), \end{aligned} \tag{22}$$

although the A–A singular term is zero. However, within the APY approximation, c_{ij}^{AA}, c_{ij}^{BB}, and c_{ij}^{BB} all vanish beyond the corresponding hard-core diameter: $c_{ij}^{\alpha\beta,\mathrm{reg}}(r) = 0$ when $r > \sigma_{\alpha\beta}$. As can be demonstrated from the Baxter equations for DCF's of Eqs. (12), this fact in turn implies that the functions $q_{ij}^{\alpha\beta}(r)$ have the same property[35,36]

$$q_{ij}^{\alpha\beta}(r) = 0 \quad \text{for}\ \ r > \sigma_{\alpha\beta}\ \text{(and also for}\ r < L_{\alpha\beta}), \tag{23}$$

but without any $\delta(r-\sigma_{\alpha\beta})$ singularity. Consequently, the Baxter equations (12) become

$$\begin{aligned} r h_{ij}^{\alpha\beta}(|r|) = &-\left[q_{ij}^{\alpha\beta}(r)\right]' + 2\pi \sum_{\gamma}\sum_{k,\ell}\int_{L_{\alpha\gamma}}^{\sigma_{\alpha\gamma}} dz\, q_{ik}^{\alpha\gamma}(z) \\ &\times \rho_{k\ell}^{\gamma}\, h_{\ell j}^{\gamma\beta}(|r-z|)\,(r-z), \end{aligned} \tag{24}$$

for $r > L_{\alpha\beta}$, and

$$\begin{aligned} r c_{ij}^{\alpha\beta}(|r|) = &-\left[q_{ij}^{\alpha\beta}(r)\right]' + 2\pi \sum_{\gamma}\sum_{k,\ell}\frac{\partial}{\partial r} \\ &\times \int_{L_{\gamma\alpha}}^{\min(\sigma_{\gamma\alpha},\sigma_{\gamma\beta}-r)} dz\, q_{ki}^{\gamma\alpha}(z)\,\rho_{k\ell}^{\gamma}\, q_{\ell j}^{\gamma\beta}(r+z), \end{aligned} \tag{25}$$

for $L_{\alpha\beta} < r < \sigma_{\alpha\beta}$ (note that the absolute value of $|r|$ is necessary, since some $L_{\alpha\beta}$ may be negative and, consequently, in these equations r is no more a distance, but a coordinate which can assume even negative values).

Solving the Baxter equations in the present case is thus equivalent to finding the auxiliary functions $q_{ij}^{\alpha\beta}(r)$ in the interval $(L_{\alpha\beta},\sigma_{\alpha\beta})$.

C. Analytic solution

To make the paper more readable, many details of our analytic calculations are reported in the Appendices. Here, we only present the main results. Our solution to the Baxter equations consists in the following set of polynomials

$$q_{ij}^{\alpha\beta}(r) = \begin{cases} \left[\frac{1}{2}a_i^{\alpha}\left(r^2-\sigma_{\alpha\beta}^2\right) + b_i^{\alpha}\left(r-\sigma_{\alpha\beta}\right)\right]\,\delta_{j0} + K_{ij}^{\alpha\beta}\sigma_{\alpha\beta}^2 & L_{\alpha\beta} \leq r \leq \sigma_{\alpha\beta}, \\ 0 & \text{elsewhere}, \end{cases} \tag{26}$$

depending on the parameters $\left\{a_i^{\alpha}, b_i^{\alpha}, K_{ij}^{\alpha\beta}\right\}$. For $j = 1$, these functions reduce to constants, i.e., $q_{i1}^{\alpha\beta}(r) = K_{i1}^{\alpha\beta}\sigma_{\alpha\beta}^2$, and in particular $q_{i1}^{AA}(r) = 0$. As can be shown, $q_{ij}^{\alpha\beta}(r)$ must satisfy the symmetry relation[35,36]

$$q_{ij}^{\alpha\beta}(L_{\alpha\beta}) = q_{ji}^{\beta\alpha}(L_{\beta\alpha}), \tag{27}$$

while $q_{ij}^{AB}(r) \neq q_{ji}^{BA}(r)$ except for $i = j$.

Observe that the auxiliary functions $q_{ij}^{\alpha\beta}(r)$ are regular, with no δ-singularity. However, at contact q_{ij}^{AA} is continuous (with $q_{ij}^{AA}(\sigma_A) = 0$), whereas q_{ij}^{BB}, q_{ij}^{AB}, and q_{ij}^{BA} have a jump discontinuity. Recalling that the derivative of a function $f(x)$ with a jump discontinuity at x_0 must contain the contribution $\left[f(x_0^+) - f(x_0^-)\right]\,\delta(x - x_0)$, one gets

$$\left[q_{ij}^{\alpha\beta}(r)\right]' = \left(a_i^{\alpha} r + b_i^{\alpha}\right)\,\delta_{j0} - K_{ij}^{\alpha\beta}\sigma_{\alpha\beta}\,\delta(r-\sigma_{\alpha\beta}). \tag{28}$$

In other words, the $q_{ij}^{\alpha\beta}(r)$'s are regular, but their derivatives $\left[q_{ij}^{\alpha\beta}(r)\right]'$ include a singular δ-term, stemming from the discontinuities of the Baxter functions.

The constant term $K_{ij}^{\alpha\beta}\sigma_{\alpha\beta}^2$ in $q_{ij}^{\alpha\beta}(r)$ could also be deduced from the DCF's through a relationship obtained from Eq. (25), i.e.,

$$q_{ij}^{\alpha\beta}(\sigma_{\alpha\beta}^-) = \int_{\sigma_{\alpha\beta}^-}^{\infty} dz\, z c_{ij}^{\alpha\beta}(z). \tag{29}$$

With regard to the parameters $\left\{a_i^{\alpha}, b_i^{\alpha}, K_{ij}^{\alpha\beta}\right\}$, it is simple to obtain $\left\{a_i^{\alpha}, b_i^{\alpha}\right\}$ as functions of the yet undetermined $\left\{K_{ij}^{\alpha\beta}\right\}$ (see Appendix A). This solution is

$$a_i^{\alpha} = a_{\alpha}^{\mathrm{HS}}\,\delta_{i0} - \frac{X_i^{\alpha}}{\Delta}, \quad b_i^{\alpha} = b_{\alpha}^{\mathrm{HS}}\,\delta_{i0} + \frac{X_i^{\alpha}}{\Delta}\frac{\sigma_{\alpha}}{2}, \tag{30}$$

with

$$a_\alpha^{\rm HS} = \frac{1}{\Delta} + \frac{3\xi_2\sigma_\alpha}{\Delta^2}, \quad b_\alpha^{\rm HS} = -\frac{3\xi_2\sigma_\alpha^2}{2\Delta^2}, \tag{31}$$

$$\xi_m = \sum_\alpha \xi_m^\alpha, \qquad \xi_m^\alpha = \frac{\pi}{6}\rho_\alpha\sigma_\alpha^m, \tag{32}$$

$$X_i^\alpha = \sum_\gamma X_i^{\alpha\gamma}, \quad X_i^{\alpha\gamma} = 2\pi\rho_\gamma\sigma_\gamma\sigma_{\alpha\gamma}^2\left(K_{i0}^{\alpha\gamma} + x_0^\gamma K_{i1}^{\alpha\gamma}\right), \tag{33}$$

where $\Delta = 1-\eta$, and $\eta \equiv \xi_3$ is the total volume fraction of all particles. Observe that the ξ_m's depend only on the total densities $\{\rho_A, \rho_B\}$, i.e., they are independent of the actual number of unbound monomers. Moreover, $X_i^{\alpha\gamma}$ represents the contribution of all attractive forces (surface adhesion and/or chemical association) added to the HS repulsion in the interaction between monomers of species α and γ.

In our SJD model, from the definitions (18) and (21) for $\left\{K_{ij}^{\alpha\beta}\right\}$ it follows that

$$\begin{cases} X_0^A = 0, & X_1^A = X_1^{AB} = \mathcal{M}^{AB}, \\ X_0^B = X_0^{BB} = \Lambda_0, & X_1^B = X_1^{BB} + X_1^{BA} = \Lambda_1 + \mathcal{M}^{BA}, \end{cases} \tag{34}$$

where the quantities

$$\Lambda_i = 12\eta_B\left(\lambda_{i0} + x_0^B\lambda_{i1}\right) \tag{35}$$

($\eta_\alpha \equiv \xi_3^\alpha$ is a partial volume fraction only due to particles of species α) stem from the B–B sticky interaction, while

$$\begin{aligned} \mathcal{M}^{AB} &= 12\xi_1^B\sigma_{AB}^2\, x_0^B\mathcal{B}, \\ \mathcal{M}^{BA} &= 12\xi_1^A\sigma_{BA}^2\, x_0^A\mathcal{B} \end{aligned} \tag{36}$$

are related to the chemical bonding between unlike monomers. We will now study $\mathcal{M}^{AB}$ and $\mathcal{M}^{BA}$ in more depth.

D. Chemical equilibrium

For the chemical equilibrium $A + B \rightleftarrows AB$ the law of mass action reads as

$$\frac{\rho_{AB}}{\rho_0^A\rho_0^B} = \mathcal{K}_{\rm eq}, \tag{37}$$

where $\rho_{AB} \equiv \rho_{\rm dim}$ is the density of dimers, and $\mathcal{K}_{\rm eq}$ is the equilibrium constant. Then, in the case of an equimolar starting mixture, one finds

$$\rho_1^A = \rho_1^B = \rho_{AB} = \rho_0^A\rho_0^B\,\mathcal{K}_{\rm eq}, \tag{38}$$

which leads to

$$\begin{cases} \rho_A = \rho_0^A + \rho_1^A = \rho_0^A + \rho_0^A\rho_0^B\,\mathcal{K}_{\rm eq}, \\ \rho_B = \rho_0^B + \rho_1^B = \rho_0^B + \rho_0^B\rho_0^A\,\mathcal{K}_{\rm eq}. \end{cases} \tag{39}$$

This is the origin of the self-consistent relationship between ρ_0^α and ρ_α previously given in Eq. (9). Comparing Eqs. (9) and (39) leads to conclude that

$$\mathcal{K}_{\rm eq} = \int d\mathbf{r}\, f_b^{AB}(r) g_{00}^{AB}(r). \tag{40}$$

For our SJD model, where chemical bonding is described by a peculiar sticky interaction, i.e., the SHS* potential, $f_b^{AB}(r)$ must be replaced by $f_{AB}^{\rm SHS^*}(r)$ of Eqs. (14), so that

$$\mathcal{K}_{\rm eq} = 4\pi\sigma_{AB}^3\, k_{\rm chem}\, y_{00}^{AB}(\sigma_{AB}) = 4\pi\sigma_{AB}^3\,\mathcal{B}. \tag{41}$$

Putting $\rho_0^B = \rho_0^A$ into the first of Eqs. (39) and solving the resulting quadratic equation for ρ_0^A, the physically significant root reads as

$$\rho_0^A = \frac{\sqrt{1+4\mathcal{K}_{\rm eq}\rho_A}-1}{2\mathcal{K}_{\rm eq}} = \frac{\rho_A}{\frac{1}{2}\left[1+\sqrt{1+4\mathcal{K}_{\rm eq}\rho_A}\right]}, \tag{42}$$

which implies that

$$x_0^A = x_0^B = \frac{1}{\frac{1}{2}\left[1+\sqrt{1+4\mathcal{K}_{\rm eq}\rho_A}\right]}. \tag{43}$$

From Eqs. (41)–(43) one sees that, if the strength of the chemical association becomes infinite (i.e., $k_{\rm chem}$ and $\mathcal{B} \to \infty$), then the equilibrium constant must diverge too, while $\rho_0^A = \rho_0^B \to 0$, $x_0^A = x_0^B \to 0$, and the molar fraction of dimers tends to unity (complete association limit). From Eqs. (39) and (41) one also gets

$$\mathcal{B} = \frac{1-x_0^A}{4\pi\sigma_{AB}^3\, x_0^A x_0^B\,\rho_A} = \frac{1-x_0^B}{4\pi\sigma_{AB}^3\, x_0^A x_0^B\,\rho_B}, \tag{44}$$

which shows that $\mathcal{B}$ diverges as $\left(x_0^A x_0^B\right)^{-1} = \left(x_0^A\right)^{-2}$ when $x_0^A = x_0^B \to 0$ (since the two numerators tend to $\rho_A = \rho_B \neq 0$). Furthermore, these expressions for $\mathcal{B}$ allow us to re-express $\mathcal{M}^{AB}$ and $\mathcal{M}^{BA}$ in the simpler form

$$\mathcal{M}^{AB} = \frac{1-x_0^B}{x_0^A}\mathcal{D}_B, \qquad \mathcal{M}^{BA} = \frac{1-x_0^A}{x_0^B}\mathcal{D}_A, \tag{45}$$

where

$$\mathcal{D}_\alpha = \frac{\sigma_\alpha}{2\sigma_{AB}} = \frac{\sigma_\alpha}{\sigma_A+\sigma_B}. \tag{46}$$

The expressions for $\{a_i^\alpha, b_i^\alpha\}$ then become

$$\begin{aligned} a_0^A &= a_A^{\rm HS}, & b_0^A &= b_A^{\rm HS}, \\ a_1^A &= -\frac{1}{\Delta}\frac{x_{\rm dim}}{x_0^A}(1-\mathcal{R}), & b_1^A &= -\frac{1}{2}a_1^A\sigma_A, \\ a_0^B &= a_B^{\rm HS} - \frac{\Lambda_0}{\Delta}, & b_0^B &= b_B^{\rm HS} + \frac{1}{2}\frac{\Lambda_0}{\Delta}\sigma_B, \\ a_1^B &= -\frac{1}{\Delta}\left(\Lambda_1 + \frac{x_{\rm dim}}{x_0^B}\mathcal{R}\right), & b_1^B &= -\frac{1}{2}a_1^B\sigma_B, \end{aligned} \tag{47}$$

where $x_{\rm dim} = 1 - x_0^A = 1 - x_0^B$ is the molar fraction of the dimers, and

$$\begin{aligned} \mathcal{R} &= (1+\sigma_B/\sigma_A)^{-1} = \mathcal{D}_A, \\ 1-\mathcal{R} &= 1-\mathcal{D}_A = \mathcal{D}_B, \end{aligned} \tag{48}$$

take into account the size ratio of the monomers forming the dumbbell (in the case of equal diameters, the counterpart of $\mathcal{R}x_{\rm dim}$ was denoted as $2Y$ in Ref. 37). More precisely, $\mathcal{R} \equiv \mathcal{R}_{\rm HS}$ is a rough measure of the HS portion of the dumbbell surface, and takes values in the interval $[0,1]$, while $\mathcal{R}_{\rm SHS} = 1 - \mathcal{R}_{\rm HS}$ refers to the adhesive part. In particular,

$$\mathcal{R} \to \begin{cases} 1 & \text{if } \sigma_B \to 0 \quad \text{(HS limit, 100\% HS)} \\ \dfrac{1}{2} & \text{if } \sigma_B \to \sigma_A, \\ 0 & \text{if } \sigma_B \to \infty \text{ or } \sigma_A \to 0 \quad \text{(SHS limit, 0\% HS).} \end{cases} \tag{49}$$

Thus, $\frac{1}{2} < \mathcal{R} \le 1$ means that the HS fraction of the dumbbell surface is larger than the SHS one, whereas $0 \le \mathcal{R} < \frac{1}{2}$ corresponds to the predominance of the sticky contribution. Note that η_B can be obtained from η through the relation

$$\eta_B = \frac{(1-\mathcal{R})^3}{\mathcal{R}^3 + (1-\mathcal{R})^3}\,\eta. \tag{50}$$

With regard to Eqs. (45)–(47), a very important remark is that both $\mathcal{M}^{AB}$ and $\mathcal{M}^{BA}$, as well as all a_1^α and b_1^α, diverge like $\left(x_0^A\right)^{-1}$ or $\left(x_0^B\right)^{-1}$ in the limit of complete association. Such a finding is, however, not worrying. In fact, as assumed by Wu and Chiew,[37] the significant quantity is the whole function $q_{\alpha\beta}(r)$, rather than its separate components. Since

$$\begin{aligned} q_{\alpha\beta}(r) &= q_{00}^{\alpha\beta}(r) + x_0^\alpha\, q_{10}^{\alpha\beta}(r) + x_0^\beta\, q_{01}^{\alpha\beta}(r) + x_0^\alpha x_0^\beta\, q_{11}^{\alpha\beta}(r) \\ &= q_{00}^{\alpha\beta}(r) + \widetilde{q}_{10}^{\alpha\beta}(r) + \widetilde{q}_{01}^{\alpha\beta}(r) + \widetilde{q}_{11}^{\alpha\beta}(r), \end{aligned} \tag{51}$$

where we have defined

$$\widetilde{q}_{ij}^{\alpha\beta}(r) = \left(x_0^\alpha\right)^{\delta_{i1}}\, q_{ij}^{\alpha\beta}(r)\, \left(x_0^\beta\right)^{\delta_{j1}}, \tag{52}$$

the important functions are the $\widetilde{q}_{ij}^{\alpha\beta}$'s, which include the weight-factors related to the molar fractions. Although some $q_{ij}^{\alpha\beta}$ diverge in the limit of complete association, the weighted components $\widetilde{q}_{ij}^{\alpha\beta}$ remain finite. Note that the same behavior is found for $h_{\alpha\beta}$, $h_{ij}^{\alpha\beta}$, $\widetilde{h}_{ij}^{\alpha\beta}$, and $g_{\alpha\beta}$,

$$g_{\alpha\beta}(r) = 1 + h_{00}^{\alpha\beta}(r) + \widetilde{h}_{10}^{\alpha\beta}(r) + \widetilde{h}_{01}^{\alpha\beta}(r) + \widetilde{h}_{11}^{\alpha\beta}(r). \tag{53}$$

In particular, we will also consider

$$\widetilde{\lambda}_{00} = \lambda_{00}, \quad \widetilde{\lambda}_{10} = x_0^A\, \lambda_{10}, \quad \widetilde{\lambda}_{11} = x_0^A\, \lambda_{11}\, x_0^B, \tag{54}$$

with $x_0^A = x_0^B$.

III. SOLUTION FOR PURE SJD FLUIDS

The final solution for a pure fluid containing only sticky Janus dumbbells can now be obtained by taking the *complete association limit*, i.e., $x_0^A = x_0^B \to 0$, and consequently $x_{\rm dim} \to 1$. In the following, instead of Eq. (52), we thus assume that

$$\widetilde{q}_{ij}^{\alpha\beta}(r) = \lim_{x_0^A = x_0^B \to 0} \left(x_0^\alpha\right)^{\delta_{i1}}\, q_{ij}^{\alpha\beta}(r)\, \left(x_0^\beta\right)^{\delta_{j1}}. \tag{55}$$

A similar definition applies to all other quantities with a tilde. However, for simplicity, we will continue to write λ_{00} instead of the more correct $\widetilde{\lambda}_{00}$ $(= \lim_{x_0^A = x_0^B \to 0} \lambda_{00})$.

After recalling that

$$q_{\alpha\beta}^{\rm HS}(r) = \frac{1}{2} a_\alpha^{\rm HS}\left(r^2 - \sigma_{\alpha\beta}^2\right) + b_\alpha^{\rm HS}\left(r - \sigma_{\alpha\beta}\right), \quad \text{for } L_{\alpha\beta} \le r \le \sigma_{\alpha\beta}, \tag{56}$$

we hereafter collect all final results for the partial contributions $\widetilde{q}_{ij}^{\alpha\beta}(r)$ of our SJD model,

(i) For A–A pairs

$$\begin{cases} \widetilde{q}_{00}^{AA}(r) = q_{AA}^{\rm HS}(r), \\ \widetilde{q}_{10}^{AA}(r) = -\dfrac{1}{2\Delta}\,(1-\mathcal{R})\; r\,(r-\sigma_A), \\ \widetilde{q}_{01}^{AA}(r) = 0, \\ \widetilde{q}_{11}^{AA}(r) = 0, \end{cases} \qquad 0 \le r \le \sigma_A. \tag{57}$$

(ii) For B–B pairs

$$\begin{cases} \widetilde{q}_{00}^{BB}(r) = q_{BB}^{\rm HS}(r) - \dfrac{1}{2\Delta}\widetilde{\Lambda}_0\, r\,(r-\sigma_B) + \lambda_{00}\sigma_B^2, \\ \widetilde{q}_{10}^{BB}(r) = -\dfrac{1}{2\Delta}\left(\widetilde{\Lambda}_1 + \mathcal{R}\right)\; r\,(r-\sigma_B) + \widetilde{\lambda}_{10}\sigma_B^2, \\ \widetilde{q}_{01}^{BB}(r) = \widetilde{\lambda}_{01}\sigma_B^2, \\ \widetilde{q}_{11}^{BB}(r) = \widetilde{\lambda}_{11}\sigma_B^2, \end{cases} \qquad 0 \le r < \sigma_B, \tag{58}$$

where

$$\begin{aligned} \widetilde{\Lambda}_0 &= 12\eta_B\left(\lambda_{00} + \widetilde{\lambda}_{10}\right), \\ \widetilde{\Lambda}_1 &= 12\eta_B\left(\widetilde{\lambda}_{10} + \widetilde{\lambda}_{11}\right). \end{aligned} \tag{59}$$

(iii) In the A–B case

$$\begin{cases} \widetilde{q}_{00}^{AB}(r) = q_{AB}^{\mathrm{HS}}(r), \\ \widetilde{q}_{10}^{AB}(r) = -\dfrac{1}{2\Delta}(1-\mathcal{R})\ (r-L_{AB})(r-\sigma_{AB}), \\ \widetilde{q}_{01}^{AB}(r) = 0, \\ \widetilde{q}_{11}^{AB}(r) = (12\xi_1)^{-1}, \end{cases} \quad L_{AB} \le r < \sigma_{AB}. \tag{60}$$

(iv) In the B–A case

$$\begin{cases} \widetilde{q}_{00}^{BA}(r) = q_{BA}^{\mathrm{HS}}(r) - \dfrac{1}{2\Delta}\widetilde{\Lambda}_0\ (r-L_{BA})(r-\sigma_{AB}), \\ \widetilde{q}_{10}^{BA}(r) = -\dfrac{1}{2\Delta}\left(\widetilde{\Lambda}_1+\mathcal{R}\right)\ (r-L_{BA})(r-\sigma_{AB}), \\ \widetilde{q}_{01}^{BA}(r) = 0, \\ \widetilde{q}_{11}^{BA}(r) = (12\xi_1)^{-1}, \end{cases} \quad L_{BA} \le r < \sigma_{AB}. \tag{61}$$

Eqs. (57)-(61) represent our APY solution for the pure SJD fluid with arbitrary diameters. It is worth remarking that the $\widetilde{q}_{ij}^{\alpha\beta}(r)$'s depend only on the parameters $\left\{\mathcal{R}, \lambda_{00}, \widetilde{\lambda}_{10}, \widetilde{\lambda}_{11}\right\}$. Moreover, in all cases $\widetilde{q}_{01}^{\alpha\beta}(r)$ and $\widetilde{q}_{11}^{\alpha\beta}(r)$ are constant.

Starting from the knowledge of these Baxter factor correlation functions it is possible, in principle, to compute all structural and thermodynamic properties of our heteronuclear dimer fluid.[37,38] In particular, the total correlation functions $\widetilde{h}_{ij}^{\alpha\beta}(r)$ can be obtained through Perram's iteration method.[37,39] Such a numerical and analytical work on heteronuclear SJD structure and thermodynamics will be deferred to a forthcoming publication.

IV. FULLY ANALYTIC EXPRESSIONS FOR THE λ_{ij} PARAMETERS

A. Nonlinear system for arbitrary diameters

Now, the only yet undetermined quantities in the expressions (47) for $\left\{a_i^\alpha, b_i^\alpha\right\}$ remain $\widetilde{\Lambda}_0$ and $\widetilde{\Lambda}_1$. The determination of the stickiness parameters $\lambda_{ij} = t\ y_{ij}^{BB}(\sigma_{\alpha\beta})$ requires the knowledge of the contact values of the B–B cavity correlation functions. As shown in Appendix B, item (a), the APY partial cavity correlation functions at contact are given by

$$y_{ij}^{\alpha\beta}(\sigma_{\alpha\beta}) = y_{\alpha\beta}^{\mathrm{HS}}(\sigma_{\alpha\beta})\delta_{i0}\delta_{j0} - \frac{1}{\Delta}\frac{X_i^\alpha\sigma_\beta\delta_{j0} + X_j^\beta\sigma_\alpha\delta_{i0}}{2\sigma_{\alpha\beta}} + \frac{2\pi}{\sigma_{\alpha\beta}}\sum_\gamma\sum_{k,\ell}\left(K_{ik}^{\alpha\gamma}\sigma_{\alpha\gamma}^2\right)\ \rho_{k\ell}^\gamma\ \left(K_{\ell j}^{\gamma\beta}\sigma_{\gamma\beta}^2\right), \tag{62}$$

where

$$y_{\alpha\beta}^{\mathrm{HS}}(\sigma_{\alpha\beta}) = \frac{1}{\Delta} + \frac{3\xi_2}{2\Delta^2}\frac{\sigma_\alpha\sigma_\beta}{\sigma_{\alpha\beta}} \tag{63}$$

is the PY approximation to the HS cavity functions.

Applying Eq. (62) to the B–B case, and replacing $y_{ij}^{BB}(\sigma_B)$ with $t^{-1}\lambda_{ij}$, yields three coupled quadratic equations for $\left\{\lambda_{00}, \widetilde{\lambda}_{10} = \widetilde{\lambda}_{01}, \widetilde{\lambda}_{11}\right\}$,

$$\begin{cases} 12\eta_B t\ \lambda_{00}^2 + \left(24\eta_B t\ \widetilde{\lambda}_{10} - 1 - \dfrac{12\eta_B t}{\Delta}\right)\lambda_{00} + t\ y_{BB}^{\mathrm{HS}} - \dfrac{12\eta_B t}{\Delta}\widetilde{\lambda}_{10} = 0, \\ 12\eta_B t\ \widetilde{\lambda}_{10}^2 - \widetilde{\lambda}_{10} + 12\eta_B t\left(\lambda_{00} - \dfrac{1}{2\Delta}\right)\left(\widetilde{\lambda}_{10} + \widetilde{\lambda}_{11}\right) - \dfrac{1}{2\Delta}\mathcal{R}t\ x_{\mathrm{dim}} = 0, \\ \left(1 - 24\eta_B t\ \widetilde{\lambda}_{10}\right)\widetilde{\lambda}_{11} = 12\eta_B t\ \widetilde{\lambda}_{10}^2. \end{cases} \tag{64}$$

Moreover, the equation for $\widetilde{\lambda}_{01}$ obtained from Eq. (62) is exactly the same as the second of Eqs. (64). Hereafter, we will, however, assume that $x_{\mathrm{dim}} = 1$ (complete association limit).

From the last of Eqs. (64), one finds by direct substitution that $\widetilde{\lambda}_{10}$ cannot be equal to $(24\eta_B t)^{-1}$. Consequently, $\widetilde{\lambda}_{11}$ can be derived from $\widetilde{\lambda}_{10}$ as

$$\widetilde{\lambda}_{11} = \frac{12\eta_B t\ \widetilde{\lambda}_{10}^2}{1 - 24\eta_B t\ \widetilde{\lambda}_{10}}. \tag{65}$$

By exploiting this expression, the first two of Eqs. (64) become a system with only two unknowns, i.e.,

$$\begin{cases} 12\eta_B t\ \lambda_{00}^2 + \left(24\eta_B t\ \widetilde{\lambda}_{10} - 1 - \dfrac{12\eta_B t}{\Delta}\right)\lambda_{00} + t\ y_{BB}^{\mathrm{HS}} - \dfrac{12\eta_B t}{\Delta}\widetilde{\lambda}_{10} = 0, \\ \left(12\eta_B t\ \widetilde{\lambda}_{10}^2 - \widetilde{\lambda}_{10}\right)\left[1 + 12\eta_B t\left(\lambda_{00} - \dfrac{1}{2\Delta}\right)\left(24\eta_B t\ \widetilde{\lambda}_{10} - 1\right)^{-1}\right] - \dfrac{1}{2\Delta}\mathcal{R}t = 0. \end{cases} \tag{66}$$

In the case of equal diameters, Wu and Chiew[37] followed the method by Weist and Glandt[19] and were able to decouple this system, obtaining two separate fourth-degree polynomial equations in each of λ_{00} and $\widetilde{\lambda}_{10}$. Such algebraic equations were then solved numerically. Among their four (in general complex) roots for λ_{00} (or for $\widetilde{\lambda}_{10}$), these authors chose the only physically significant one by checking which real root satisfies the correct zero-density limit. For our model, from Eqs. (64) the zero-density conditions read as

$$\lim_{\eta\to 0}\lambda_{00}=t,\qquad \lim_{\eta\to 0}\widetilde{\lambda}_{10}=-\frac{1}{2}\mathcal{R}t,$$

and

$$\lim_{\eta\to 0}\widetilde{\lambda}_{11}=0. \tag{67}$$

In the present paper we solve Eqs. (66) explicitly, in a fully analytic way.

With the help of the identity

$$12\eta_B t\,\widetilde{\lambda}_{10}^2-\widetilde{\lambda}_{10}=\frac{1}{48\eta_B t}\left[\left(24\eta_B t\,\widetilde{\lambda}_{10}-1\right)^2-1\right], \tag{68}$$

and the change of variable

$$s=24\eta_B t\,\widetilde{\lambda}_{10}-1, \tag{69}$$

the system (66) is transformed into

$$\begin{cases} 12\eta_B t\,\lambda_{00}^2+\left(s-\dfrac{12\eta_B t}{\Delta}\right)\lambda_{00}+t\,y_{BB}^{\mathrm{HS}}-\dfrac{1}{2\Delta}(1+s)=0,\\ \left(s^2-1\right)\left[1+12\eta_B t\left(\lambda_{00}-\dfrac{1}{2\Delta}\right)s^{-1}\right]-\dfrac{24\eta_B\mathcal{R}t^2}{\Delta}=0. \end{cases} \tag{70}$$

The first of these equations is quadratic in λ_{00} and thus generates, for each admissible value of s, two solutions (in the complex plane), say $\lambda_{00}^{(-)}$ and $\lambda_{00}^{(+)}$. On the contrary, the second equation, linear in λ_{00}, produces a unique solution, say $\lambda_{00}^{(A)}$. Hence, the two equations of system (70) can have only one common solution, which must necessarily coincide with $\lambda_{00}^{(A)}$. Furthermore, the relationship among $\lambda_{00}^{(A)}$ and $\lambda_{00}^{(-)}$, $\lambda_{00}^{(+)}$ is not trivial. In fact, we have verified that $\lambda_{00}^{(A)}$ cannot be identified with $\lambda_{00}^{(-)}$ or $\lambda_{00}^{(+)}$ separately. As a matter of fact, $\lambda_{00}^{(A)}$ coincides with $\lambda_{00}^{(-)}$ in a η-interval just near the origin, but coincides with $\lambda_{00}^{(+)}$ in the complementary interval.

Solving the second, linear equation with respect to λ_{00} (observe that $s^2=1$ occurs only for $\eta=0$) and substituting the resulting expression $\lambda_{00}^{(A)}$ into the first of Eqs. (70) leads to an algebraic equation containing only s, while the system becomes

$$\begin{cases} \mathcal{P}(s)\equiv\mathcal{E}s^4-2\left[\mathcal{E}-2\mathcal{R}t\left(1-\dfrac{24\eta_B\mathcal{R}t^2}{\Delta}\right)\right]s^2+(\mathcal{E}-4\mathcal{R}t)=0,\\ \lambda_{00}(s)=\dfrac{1}{2\Delta}-(12\eta_B t)^{-1}\left(1-\dfrac{24\eta_B\mathcal{R}t^2}{\Delta}\,\dfrac{1}{s^2-1}\right)s, \end{cases} \tag{71}$$

where the fourth-degree polynomial $\mathcal{P}(s)$ contains only even powers of s, and

$$\begin{aligned}\mathcal{E}&=\mathcal{E}(\eta,t;\mathcal{R})\\ &=1+4\left(\mathcal{R}-\frac{1}{2}\right)\left[1-\frac{1-\mathcal{R}}{\mathcal{R}^3+(1-\mathcal{R})^3}\frac{3\eta}{2\Delta}\right]t\end{aligned} \tag{72}$$

depends on the density, temperature and/or adhesive strength, and monomer sizes.

Eq. (71) extends the analogous equation obtained by Wu and Chiew[37] for $\sigma_A=\sigma_B$ to the more general case of arbitrary diameters. We have thus obtained a *quartic* equation for $\widetilde{\lambda}_{10}$, which assumes a *biquadratic* form when expressed in terms of s, i.e., it is quadratic in the variable s^2. Finding the roots of this peculiar quartic equation is easy: one first solves for s^2, and then returns to the original unknown $\widetilde{\lambda}_{10}$. In the complex plane, the biquadratic equation has always four roots forming two pairs of conjugate solutions, whereas in the real field the number of its roots may be 4, 2, or 0. The character and behavior of these roots depend on the function $\mathcal{E}(\eta,t;\mathcal{R})$ (for $\sigma_A=\sigma_B$, one gets $\mathcal{E}=1$). In the particular case $\mathcal{E}=0$, the quartic equation reduces to $s^2=\left(1-\frac{24\eta_B\mathcal{R}t^2}{\Delta}\right)^{-1}$. For $\mathcal{E}\neq 0$ the solutions of $\mathcal{P}(s)=0$ are

$$\begin{cases} s^2=W_+\\ s^2=W_- \end{cases}, \tag{73}$$

with

$$W_\pm=1+\frac{2\mathcal{R}t}{\mathcal{E}}\left[\pm\sqrt{D}-\left(1-\frac{24\eta_B\mathcal{R}t^2}{\Delta}\right)\right], \tag{74}$$

$$D=\left(1-\frac{24\eta_B\mathcal{R}t^2}{\Delta}\right)^2+\frac{24\eta_B t}{\Delta}\mathcal{E}. \tag{75}$$

Further useful relationships are

$$W_+ - W_- = \frac{4\mathcal{R}t}{\mathcal{E}}\sqrt{D} \quad \text{and} \quad W_-W_+ = 1 - \frac{4\mathcal{R}t}{\mathcal{E}}. \tag{76}$$

Eqs. (73) say that our quartic equation splits into two quadratic equations. The explicit expressions for their (generally complex) roots are

$$\begin{cases} s_1 = -\sqrt{W_+}, & s_4 = -s_1 = \sqrt{W_+} \\ s_2 = -\sqrt{W_-}, & s_3 = -s_2 = \sqrt{W_-} \end{cases}. \tag{77}$$

Here, s_4 and s_3 may be regarded as conjugate to s_1 and s_2, respectively. Since we are only interested in real roots, besides assuming $D \geq 0$ we should establish when W_- and W_+ are non-negative.

When W_- and W_+ are both positive (which occurs for $\mathcal{E} > 4\mathcal{R}t$, or even for appropriate $\mathcal{E} < 0$), all roots are real. If $\mathcal{E} > 4\mathcal{R}t$, these are ordered as $s_1 < s_2 < s_3 < s_4$ (since $W_- < W_+$ by the first of Eqs. (76)); on the other hand, if $\mathcal{E} < 0$ the inversion $W_- > W_+$ implies that all roots are real providing that $W_+ > 0$, but now with the different ordering $s_2 < s_1 < s_4 < s_3$.

The case $W_- = 0$ (i.e., $\mathcal{E} = 4\mathcal{R}t$) corresponds to a merging and simultaneous vanishing of s_2 and s_3. Finally, when W_- is negative the roots s_2 and s_3 are complex and only two real roots survive, i.e., s_1 and $s_4 = -s_1$.

In principle, s_1 and s_2 will merge whenever a volume fraction $\eta_D(t;\mathcal{R})$ exists where D vanishes and, consequently, $W_- = W_+$. For $\eta = \eta_D$ the curves $s_1(\eta)$ and $s_2(\eta)$ must touch each other. We have numerically verified that such a contact may occur in two different ways:

(i) for $0.75 \lesssim \mathcal{R} < 1$ (predominance of HS repulsion over SHS attraction), whenever η_D exists it assumes very large values, far away from the fluid regimes we are concerned with. For $\eta = \eta_D$ four real roots meet in pairs ($s_2 = s_1$ and $s_4 = s_3$), however without crossing each other. Indeed, beyond this volume fraction all roots become complex, since $D < 0$ for $\eta > \eta_D$.

(ii) On the other hand, for $0 < \mathcal{R} \lesssim 0.25$ (predominance of SHS attraction over HS repulsion) η_D exists at low temperature and has relatively small values, lower than 0.1. Now D has a double root for $\eta = \eta_D$, being otherwise positive. Thus η_D can be determined analytically as: $\eta_D(t;\mathcal{R}) = \{1 + C_B\,[2(1-\mathcal{R})t - 1]\}^{-1}$ with $C_B = (1-\mathcal{R})^3\left[\mathcal{R}^3 + (1-\mathcal{R})^3\right]^{-1}$, provided that $t > \frac{1}{2}(1-\mathcal{R})^{-1}$ (i.e., $\tau < \frac{1}{6}(1-\mathcal{R})$). In this case, the curves $s_1(\eta)$ and $s_2(\eta)$ (as well as $s_3(\eta)$ and $s_4(\eta)$) still touch each other for $\eta = \eta_D$ but, at variance with case (i), all real roots continue to exist beyond η_D. A true crossover between s_1 and s_2 would imply an inversion of ordering, i.e., if $s_2 < s_1$ for $\eta < \eta_D$ then $s_2 > s_1$ for $\eta > \eta_D$. In fact, this never occurs; however, if one requires the continuity of both the physically meaningful root and its derivative as a function of η, then it is necessary to swap from one root to the other beyond η_D.

Coming back to the complex plane, the four $\{s_m\}$-roots determine *four* corresponding values for each stickiness parameter, i.e.,

$$\widetilde{\lambda}_{10}(s_m) = \frac{1}{24\eta_B t}(1 + s_m) \qquad (m = 1,\ldots,4), \tag{78}$$

$$\widetilde{\lambda}_{11}(s_m) = -\frac{1}{48\eta_B t}\frac{(1+s_m)^2}{s_m}, \tag{79}$$

$$\lambda_{00}(s_m) = \frac{1}{2\Delta} - \frac{s_m}{12\eta_B t}\left(1 - \frac{24\eta_B}{\Delta}\frac{\mathcal{R}t^2}{s_m^2 - 1}\right). \tag{80}$$

Summarizing, the nonlinear system (64) admits *four* complex solutions $\mathcal{S}_m = \left\{\lambda_{00}, \widetilde{\lambda}_{10}, \widetilde{\lambda}_{11}\right\}_{s=s_m}$. We are, however, interested only in the real ones which satisfy the zero-density conditions, Eqs. (67). To this aim, let us investigate the zero-density behavior of each $\widetilde{\lambda}_{10}(s_m)$, by comparing each root of the $\{s_m\}$ set (assuming them to be all real) with s^{exact} near the origin $\eta = 0$. From Eq. (69) and the zero-density limit (67) of $\widetilde{\lambda}_{10}$ it results that

$$s^{\text{exact}} = -1 + 24\eta_B t\ \widetilde{\lambda}_{10}^{\text{exact}} = -1 - 12\eta_B\mathcal{R}t^2 + O(\eta^2). \tag{81}$$

Since s^{exact} is negative near the origin, the positive s_3 and s_4 cannot reproduce the physically correct trend. To discriminate between $s_1 = -\sqrt{W_+}$ and $s_2 = -\sqrt{W_-}$, it is then sufficient to consider their zero-density limits

$$\begin{aligned} &\lim_{\eta\to 0} s_1 = -1, \\ &\lim_{\eta\to 0} s_2 = -\sqrt{1 - 4\mathcal{R}t\ \mathcal{E}^{-1}(\eta = 0, t;\mathcal{R})}. \end{aligned} \tag{82}$$

Thus, we conclude that at low densities the only physically acceptable root is s_1, and the correct real solution for the stickiness parameters is always $\mathcal{S}_1$ (even when $W_- < 0$, and $\mathcal{S}_1$, $\mathcal{S}_4$ are the only real roots),

$$\lambda_{00} = \frac{1}{2\Delta} + \frac{\sqrt{W_+}}{12\eta_B t}\left(1 - \frac{24\eta_B}{\Delta}\frac{\mathcal{R}t^2}{W_+ - 1}\right), \tag{83}$$

$$\widetilde{\lambda}_{10} = \frac{1}{24\eta_B t}\left(1 - \sqrt{W_+}\right), \tag{84}$$

$$\widetilde{\lambda}_{11} = \frac{1}{48\eta_B t}\frac{\left(1 - \sqrt{W_+}\right)^2}{\sqrt{W_+}}. \tag{85}$$

We have thus completed our analytic determination of all parameters involved in the functions $q_{ij}^{\alpha\beta}(r)$ specified by Eq. (26). Since solving the Baxter integral equations for a given model is tantamount to determining the corresponding factor correlation functions, we can rightly affirm that our solution is *fully analytic*.

V. SOME NUMERICAL RESULTS

A. Real *s*-roots and stickiness parameters

Figure 1 shows the behavior of the real s-roots of the equation $\mathcal{P}(s) = 0$ with decreasing temperature, or increasing adhesive strength, for $\mathcal{R} = \frac{1}{2}$ (equal diameters). In this case, $\mathcal{E} - 4\mathcal{R}t = 1 - 2t$ becomes negative when $t > \frac{1}{2}$, i.e., for $\tau < \frac{1}{6}$. We consider two values of τ, i.e., $\tau = 0.2$ and $\tau = 0.1$ (corresponding to $t = 0.42$ and $t = 0.83$, respectively), with $\eta = 0.2$ or 0.4.

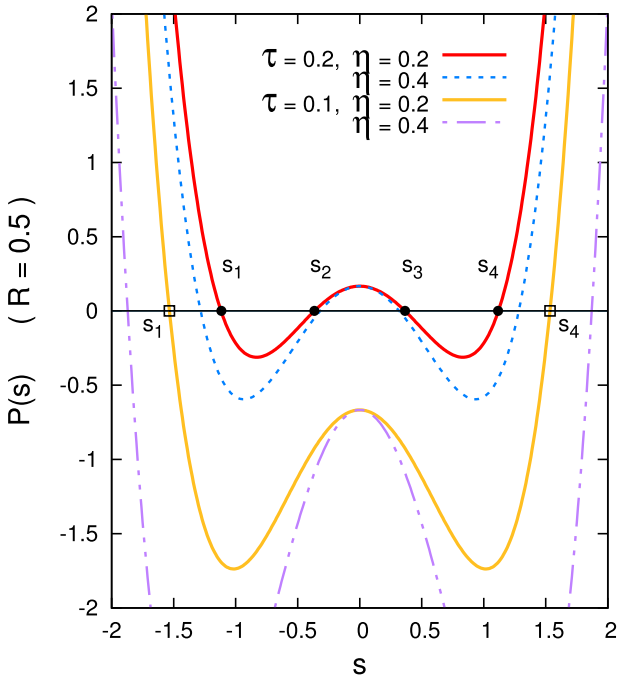

FIG. 1. Behavior of the real s-roots of the equation $\mathcal{P}(s) = 0$, for homonuclear SJD's ($\mathcal{R} = \frac{1}{2}$, equal diameters), with increasing the volume fraction η and lowering the temperature τ (or increasing the strength of the surface adhesion).

When $\tau = 0.2$ the polynomial $\mathcal{P}(s)$ has four real zeros: (s_1, s_3), together with the conjugate pair $(s_2, s_4) = (-s_3, -s_1)$. When the volume fraction η increases, these roots move as displayed in Fig. 1. On the other hand, when $\tau = 0.1$ the solutions s_2 and s_3 are complex, and we are left with two real roots, s_1 and s_4.

As proved in Section IV, it is the first real root s_1 which always determines the physically correct values of the stickiness parameters. In order to test our analytic solutions for $\left\{\lambda_{00}, \widetilde{\lambda}_{10}, \widetilde{\lambda}_{11}\right\}$, we have first solved the system of Eqs. (64) *numerically*, by using the well-known Wolfram Mathematica software. In particular, we have considered two cases among those studied by Wu and Chiew,[37] i.e., $\tau = 0.2$ and $\tau = 0.015$ (for $\sigma_A = \sigma_B$, i.e., $\mathcal{R} = \frac{1}{2}$). For their homonuclear dimer fluid these authors found, via the energy route to the equation of state, a critical temperature $\tau_c = 0.0198$ and a critical volume fraction $\eta_c = 0.228$. Thus, $\tau = 0.2$ corresponds to a supercritical case, while $\tau = 0.015$ is a subcritical value.

By visual comparison one can appreciate how our purely numerical results, plotted in Figure 2 by means of black symbols, agree with the data of Wu and Chiew reported in Figures 1, 2, and 3 of Ref. 37. At the same time, Fig. 2 clearly illustrates the full agreement between the purely numerical data and those obtained from our analytic expressions for λ_{00}, $\widetilde{\lambda}_{10}$, and $\widetilde{\lambda}_{11}$.

B. Structural information from the cavity correlation functions at contact

To conclude this paper, we try to extract some information by computing very simple quantities as the contact values of the monomer-monomer cavity correlation functions. Our aim is to compare them, qualitatively, with the overall picture on the structure of heteronuclear Janus fluids recently obtained by Munaò *et al.*[7] through MC simulations. However, we caution the reader that a strict comparison with the SW dumbbells of Ref. 7 is not immediately possible, since the attractive corona of the latter is far from being a minute fraction of the hard core.

For the SJD model within the APY closure, we get from the general relationship (19) between RDF's and cavity correlation functions, $g_{\alpha\beta}(r) = y_{\alpha\beta}(r) \exp[-\beta u_{\alpha\beta}(r)]$, and Eqs. (14): $g_{\alpha\beta}(r) = 0$ for $r < \sigma_{\alpha\beta}$, as well as

$$\begin{cases} g_{AA}(r) = y_{AA}(r) & \text{for} \quad r \geq \sigma_A, \\ g_{AB}(r) = y_{AB}(r) & r \geq \sigma_{AB}, \\ g_{BB}(r) = t\ [\sigma_B y_{BB}(\sigma_B)]\ \delta(r - \sigma_B) + y_{BB}(r) & r \geq \sigma_B. \end{cases} \tag{86}$$

Outside the core, $g_{BB}(r)$ has both a "regular" part, $y_{BB}(r)$, and a "singular" part, containing a δ-singularity and stemming from the sticky B–B surface interaction. While the RDFs have a discontinuity at the core distance, and $g_{BB}(r)$ is not even a conventional function, the $y_{\alpha\beta}(r)$'s are continuous functions.

Analytic expressions for the cavity correlation functions at contact can be derived from Eq. (62) and the relationship $\widetilde{y}_{ij}^{BB}(\sigma_B) = t^{-1}\widetilde{\lambda}_{ij}$. Here, we just present our final results,

$$\begin{aligned} y_{AA}(\sigma_A) &= y_{AA}^{\mathrm{HD}}(\sigma_A), \\ y_{AB}(\sigma_{AB}) &= y_{AB}^{\mathrm{HD}}(\sigma_{AB}) - \frac{1}{\Delta}\left(\widetilde{\Lambda}_0 + \widetilde{\Lambda}_1\right)\mathcal{R} + 2\widetilde{\Lambda}_0(1-\mathcal{R})^2 \\ &= y_{BA}(\sigma_{BA}), \\ y_{BB}(\sigma_B) &= t^{-1}\left(\lambda_{00} + 2\widetilde{\lambda}_{10} + \widetilde{\lambda}_{11}\right) \\ &= y_{BB}^{\mathrm{HD}}(\sigma_B) - \frac{1}{\Delta}\left(\widetilde{\Lambda}_0 + \widetilde{\Lambda}_1\right) + \frac{1}{12\eta_B}\left(\widetilde{\Lambda}_0^2 + 2\widetilde{\Lambda}_0\widetilde{\Lambda}_1\right), \end{aligned} \tag{87}$$

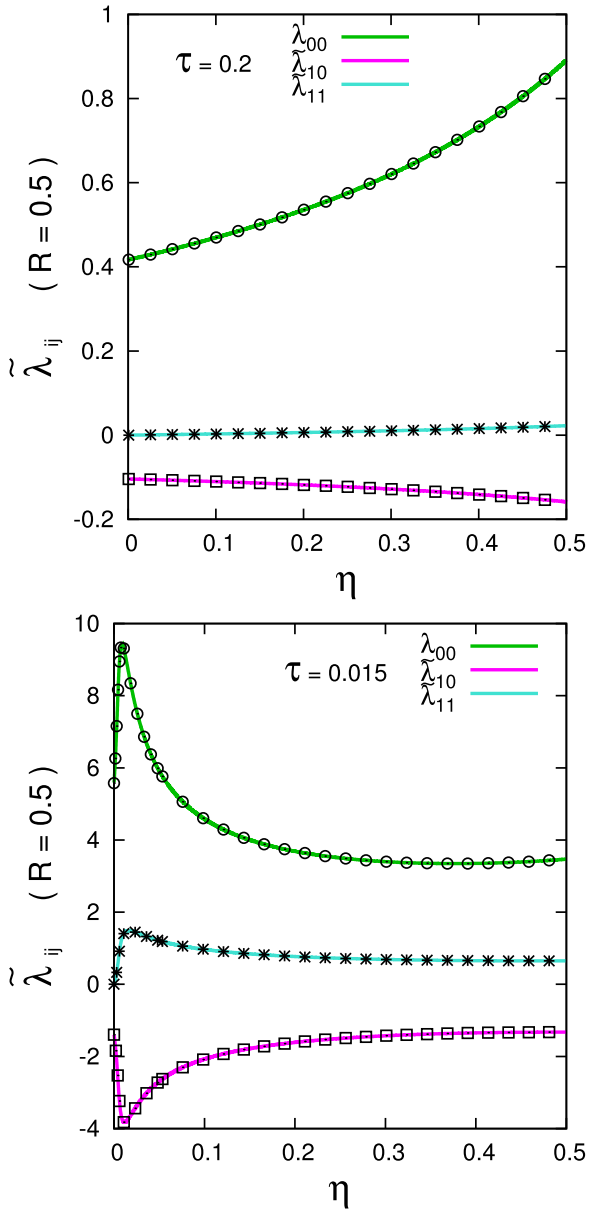

FIG. 2. Stickiness parameters $\{\lambda_{00}, \lambda_{10}, \lambda_{11}\}$ as a function of η, for homonuclear SJD's ($\mathcal{R} = \frac{1}{2}$, equal diameters), at supercritical temperature $\tau = 0.2$ (upper panel), and the subcritical one $\tau = 0.015$ (lower panel), respectively. Black symbols denote results obtained by solving the system of Eqs. (64) *fully numerically*, while solid lines are computed from our *analytic* solution, Eqs. (84)-(86).

where

$$y_{AA}^{\rm HD}(\sigma_A) = y_{AA}^{\rm HS}(\sigma_A) - \frac{1}{\Delta}(1-\mathcal{R}),$$
$$y_{AB}^{\rm HD}(\sigma_{AB}) = y_{AB}^{\rm HS}(\sigma_{AB}) - \frac{1}{\Delta}\left[\mathcal{R}^2 + (1-\mathcal{R})^2\right], \quad (88)$$
$$y_{BB}^{\rm HD}(\sigma_B) = y_{BB}^{\rm HS}(\sigma_B) - \frac{1}{\Delta}\mathcal{R}$$

refer to the corresponding hard dumbbell (HD) molecule, without surface adhesion. When $\sigma_A = \sigma_B$ these formulas reduce to those given in Ref. 37. Their zero-density limits read as

$$\lim_{\eta\to 0} y_{AA}(\sigma_A) = \mathcal{R} = \frac{\sigma_A}{\sigma_A+\sigma_B},$$
$$\lim_{\eta\to 0} y_{AB}(\sigma_{AB}) = 2\mathcal{R}(1-\mathcal{R}) = 2\frac{\sigma_A\sigma_B}{(\sigma_A+\sigma_B)^2}, \quad (89)$$
$$\lim_{\eta\to 0} y_{BB}(\sigma_B) = 1-\mathcal{R} = \frac{\sigma_B}{\sigma_A+\sigma_B}.$$

Note that, while for simple fluids $y(r)$ satisfies the condition $\lim_{\eta\to 0} y(\sigma) = 1$, here the zero-density values of the cavity functions at contact are less than unity because of the steric "screening effect" due to the remaining monomer in each of the two dumbbells.

In Figures 3-7 the monomer-monomer cavity functions at contact $y_{\alpha\beta}(\sigma_{\alpha\beta}) \equiv \overline{y}_{\alpha\beta}$ are plotted against the dimensionless density

$$\rho^* = \rho\sigma^3, \quad \text{where } \sigma = \max(\sigma_A, \sigma_B), \quad (90)$$

for five SJD models with increasing size of the SHS monomer with respect to the HS one: $\sigma_B = \frac{1}{3}\sigma_A$, $\sigma_B = \frac{1}{2}\sigma_A$, $\sigma_B = \sigma_A$, and $\sigma_B = \frac{4}{3}\sigma_A$, $\sigma_B = 3\sigma_A$, corresponding to: $\mathcal{R} = 0.75, 0.67$, 0.50, and 0.43, 0.25, respectively (if $\mathcal{R}$ decreases, then the relative importance of the stickiness attraction, measured by $\mathcal{R}_{\rm SHS} = 1-\mathcal{R}$, increases). For each dumbbell geometry, we also show the effects of decreasing the temperature from $\tau = 0.2$ to a lower value.

The diameter ratios of our dumbbells correspond to almost all the cases considered by Munaò *et al.*,[7] which refer to four different densities ($\rho^* = 0.05$, 0.1, 0.2, and 0.3) and several temperatures T^*. The main difference is that in Ref. 7 the attractive monomers were surrounded by a SW potential of width $\frac{1}{2}\sigma_B$, which is rendered here through a SHS interaction, with an infinitely thin adhesive layer. Such a difference between the two models is especially significant when the SW width becomes larger than the HS diameter σ_A (i.e., when $\sigma_A \le \frac{1}{2}\sigma_B$), so that the A-monomer is fully immersed in the attractive region of the B-one. We have preliminarily verified that in the limit of hard-dumbbells our theoretical predictions quantitatively agree with MC simulations in providing the contact values of the cavity functions, for both equal and different HS diameters. For a quantitative comparison when the attractive interactions play a significant role one would also need the precise correspondence between T^* and τ, which can be obtained by matching the second virial coefficients of the two models. This topic will, however, be deferred to the next paper, since we are now interested only in a qualitative comparison.

The MC structural results from Ref. 7 can be summarized as follows:

(i) for $\sigma_B/\sigma_A < 1$, the partial structure factor $S_{BB}(k)$ exhibits a low-k peak, which becomes more pronounced as the density increases and signals the self-assembly of SW-Janus-dumbbells into nearly spherical aggregates, similar to surfactant micelles, especially at low densities and temperatures. On the other hand, $S_{BB}(k \to 0)$ remains finite, indicating that the formation of the cluster fluid suppresses the possibility of a liquid-vapor phase transition.

(ii) when $\sigma_B \approx \sigma_A$, the self-assembled structure is different: at low temperatures and moderate/high densities,

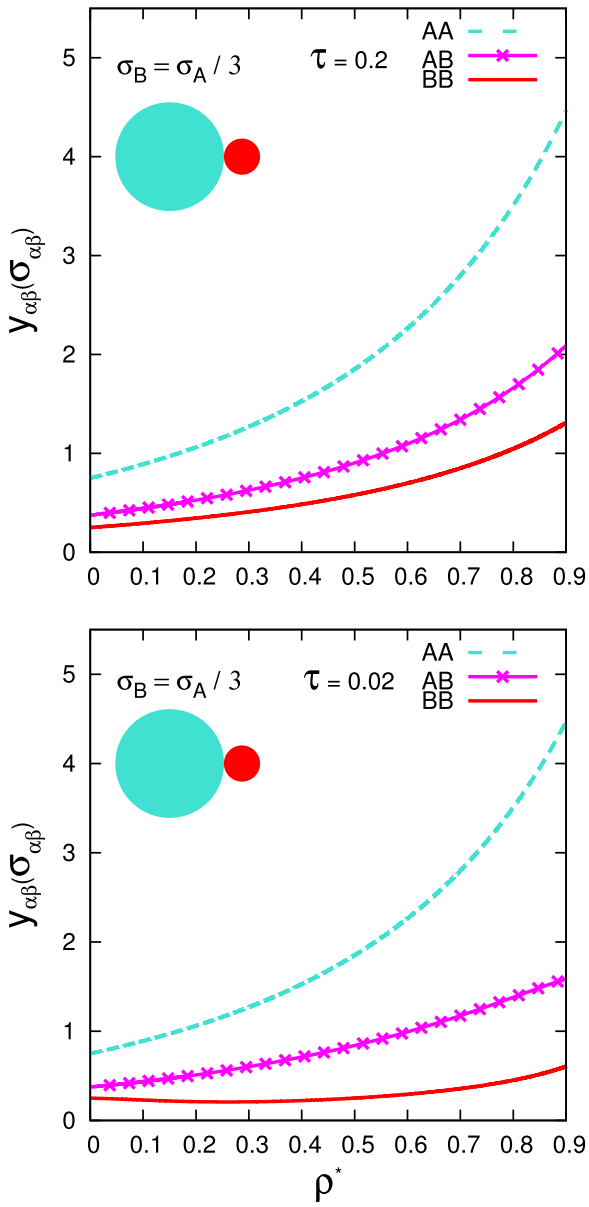

FIG. 3. Monomer-monomer cavity functions at contact, $\{\overline{y}_{AA}, \overline{y}_{AB}, \overline{y}_{BB}\}$, as functions of the dimensionless density ρ^*, for a SJD fluid with $\sigma_B = \frac{1}{3}\sigma_A$ ($\mathcal{R}_{\rm SHS} = 0.25$), at $\tau = 0.2$ (upper panel), and $\tau = 0.02$ (lower panel), respectively. The attractive monomer is B (red sphere).

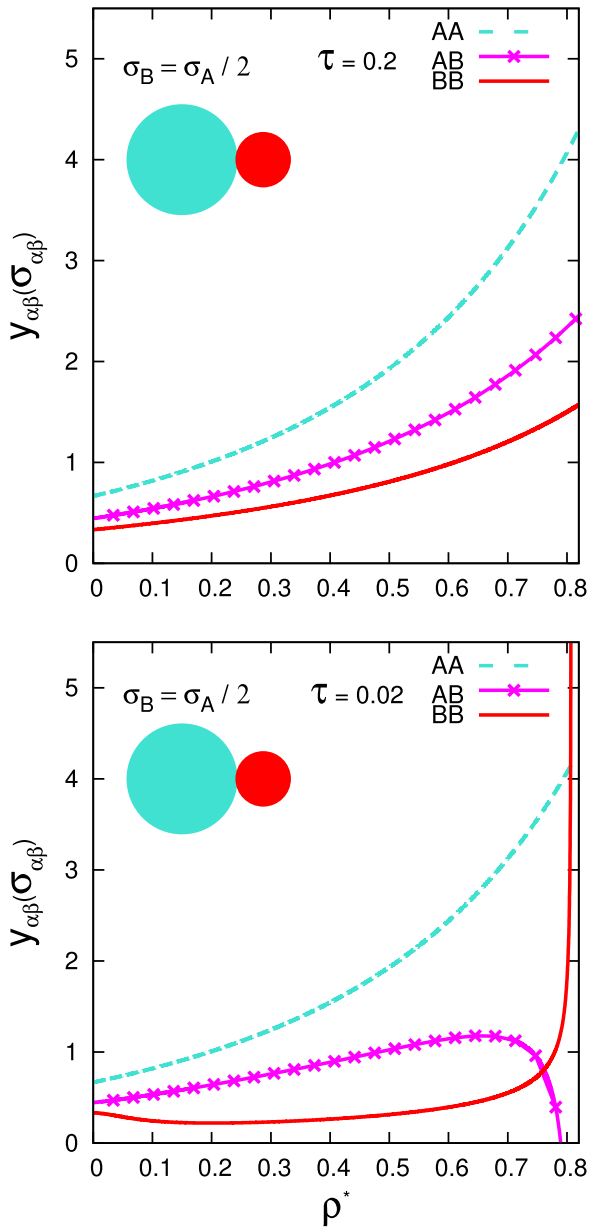

FIG. 4. Monomer-monomer cavity functions at contact, $\{\overline{y}_{AA}, \overline{y}_{AB}, \overline{y}_{BB}\}$, as functions of the dimensionless density ρ^*, for a SJD fluid with $\sigma_B = \frac{1}{2}\sigma_A$ ($\mathcal{R}_{\rm SHS} = 0.33$), at $\tau = 0.2$ (upper panel), and $\tau = 0.02$ (lower panel), respectively.

molecules would be organized into planar configurations (lamellae).

(iii) for $\sigma_B/\sigma_A > 1$, the SW interaction of width $\frac{1}{2}\sigma_B$ becomes significantly larger than the HS one (when $\sigma_A \leq \frac{1}{2}\sigma_B$, its range even extends beyond the HS diameter). Now, the MC $S_{BB}(k)$ clearly shows a diverging trend with $k \to 0$, indicating a progressive approach to a liquid-vapor phase transition, while clusters seem to disappear.

A similar scenario on the formation of micellar clusters of colloidal Janus particles comes out also from experiments and simulations by Kraft *et al.*,[40] as well as by Granick and co-workers.[41,42] Inspired by Fig. 2 of Ref. 40, we have also tried to interpret the data displayed in Figs. 3-7, by guessing some possible "contact aggregates" of SJD's, compatible with our $\overline{y}_{\alpha\beta}$-results and probably yielding a significant contribution to the correlation functions. These theoretical snapshots, given in Fig. 8, should be regarded as describing either isolated supramolecular entities or rough "building blocks" of larger aggregates. The limits of this analysis are evident to us; nevertheless, such simple images may be useful for a qualitative comparison with the structures emerging from the MC simulations.[7,40–42]

Fig. 3 refers to $\sigma_B = \frac{1}{3}\sigma_A$ ($\mathcal{R} = 0.75$, or $\mathcal{R}_{\rm SHS} = 0.25$). Both at moderate and low temperatures ($\tau = 0.2$ and 0.02, respectively), one always observes that $\overline{y}_{AA} > \overline{y}_{AB} > \overline{y}_{BB}$ over the whole, wide, interval of densities considered here. Since $\rho_A = \rho_B$, for this kind of SJD the probabilities of finding two particles at contact exhibit the same $AA > AB > BB$ order. A possible visual appearance is given in Fig. 8(a). Here,

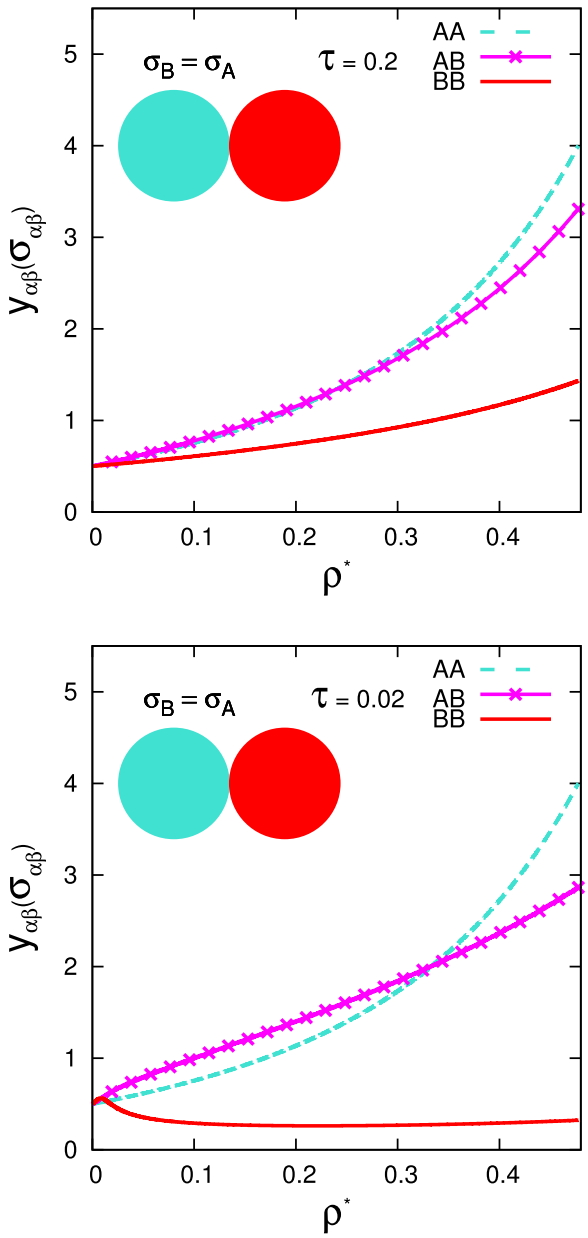

FIG. 5. Monomer-monomer cavity functions at contact, $\{\overline{y}_{AA}, \overline{y}_{AB}, \overline{y}_{BB}\}$, as functions of the dimensionless density ρ^*, for a SJD fluid with $\sigma_B = \sigma_A$ ($\mathcal{R}_{\rm SHS} = 0.50$), at $\tau = 0.2$ (upper panel), and $\tau = 0.02$ (lower panel), respectively.

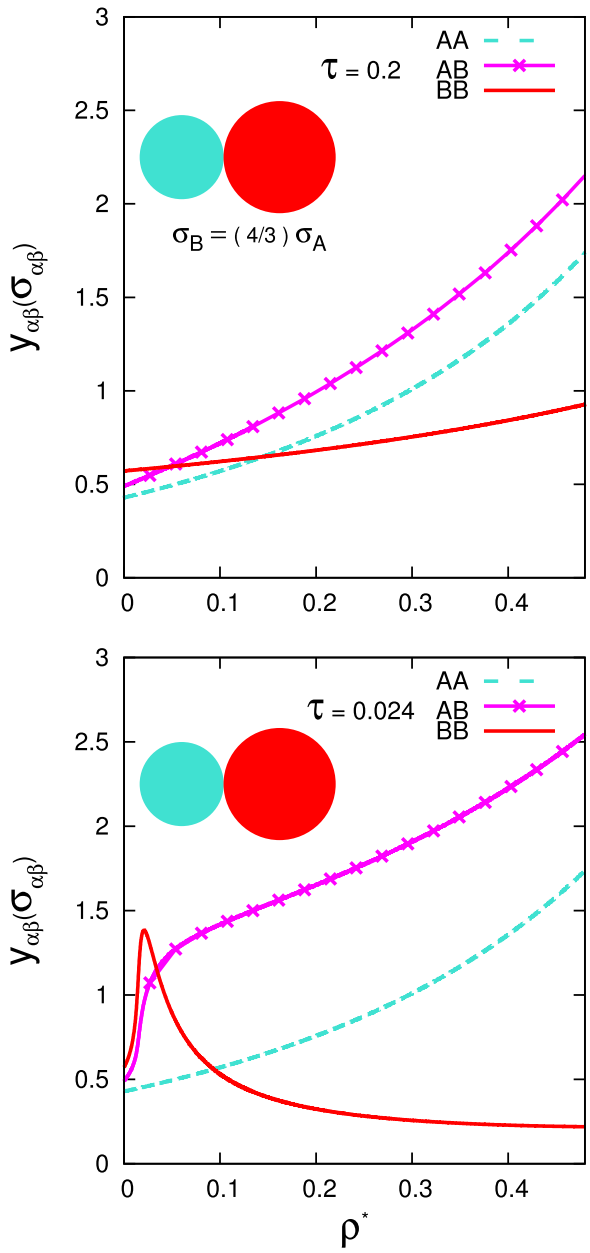

FIG. 6. Monomer-monomer cavity functions at contact, $\{\overline{y}_{AA}, \overline{y}_{AB}, \overline{y}_{BB}\}$, as functions of the dimensionless density ρ^*, for a SJD fluid with $\sigma_B = \frac{4}{3}\sigma_A$ ($\mathcal{R}_{\rm SHS} = 0.57$), at $\tau = 0.2$ (upper panel), and $\tau = 0.024$ (lower panel), respectively.

we show an aggregate of $\mathcal{N} = 4$ dumbbells. If $m_{\alpha\beta}$ denotes the numbers of contacts between α and β monomers belonging to different SJD molecules, then Fig. 8(a) corresponds to a configuration with $m_{AA} = 3 > m_{AB} = 2 > m_{BB} = 1$, compatible with the ordering $\overline{y}_{AA} > \overline{y}_{AB} > \overline{y}_{BB}$.

Upon increasing the diameter ratio σ_B/σ_A, but still keeping it below 1, we find essentially the same previous behavior for low and moderate densities, even at low temperatures. Our results agree qualitatively with part of the structural properties reported in Ref. 7. We can assess that, when $0 < \sigma_B/\sigma_A < 1$, the SJD molecules spontaneously organize into micellar clusters, in which the attractive monomers B constitute the "core" of the aggregate, while the non-attractive monomers A are located "outside."[40]

However, the bottom panel of Fig. 4 displays a rather peculiar behavior of the SJD with $\sigma_B = \frac{1}{2}\sigma_A$ ($\mathcal{R}_{\rm SHS} = 0.33$), at low temperature $\tau = 0.02$ and high densities around $\rho^* \approx 0.8$. Here, we find two singularities: $\overline{y}_{BB} \to +\infty$, and $\overline{y}_{AB} \to -\infty$. The latter divergence may be an artifact of the APY closure. In fact, it is well known that the PY approximation is inapplicable at very high densities:[43] even for simple HS's the PY $g(r)$ becomes negative for $\rho^* \gtrsim 1.18$. Our opinion is that the divergence $\overline{y}_{AB} \to -\infty$ is due to the breakdown of the closure, but seems to indicate $\overline{y}_{AB} \to 0$ as the correct trend. If this is the case, then the behavior of $\overline{y}_{BB}$ and $\overline{y}_{AB}$ may have an acceptable physical meaning. We imagine that, at very high densities, the clusters are very compressed, and the B monomers inside each "micellar core" are so ordered,

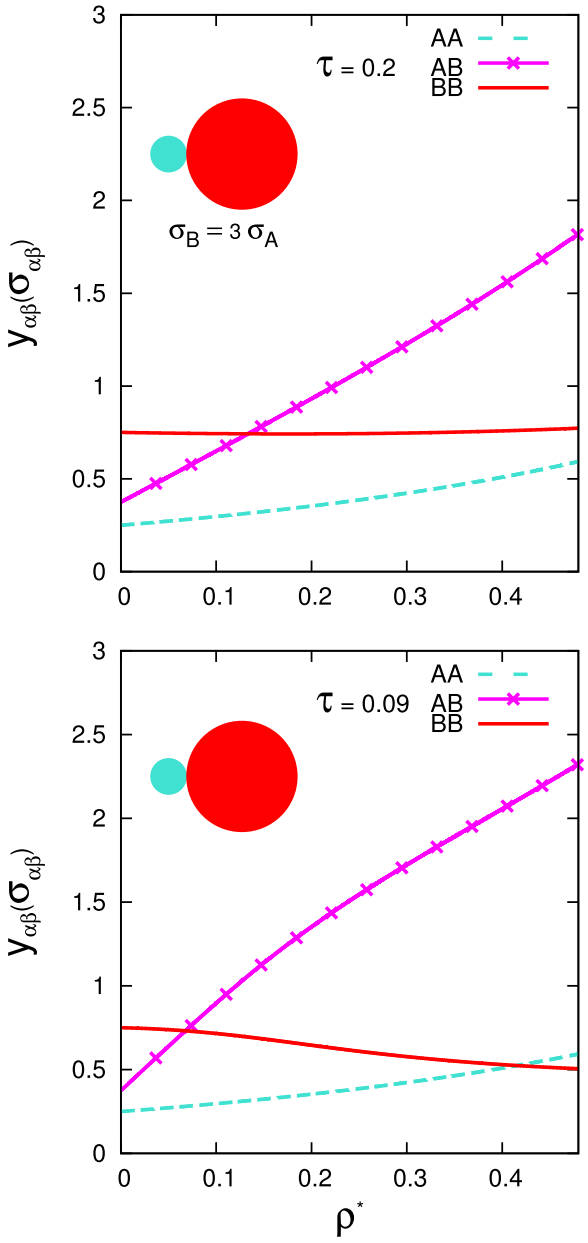

FIG. 7. Monomer-monomer cavity functions at contact, $\{\overline{y}_{AA}, \overline{y}_{AB}, \overline{y}_{BB}\}$, as functions of the dimensionless density ρ^*, for a SJD fluid with $\sigma_B = 3\sigma_A$ ($\mathcal{R}_{\rm SHS} = 0.75$), at $\tau = 0.2$ (upper panel), and $\tau = 0.09$ (lower panel), respectively.

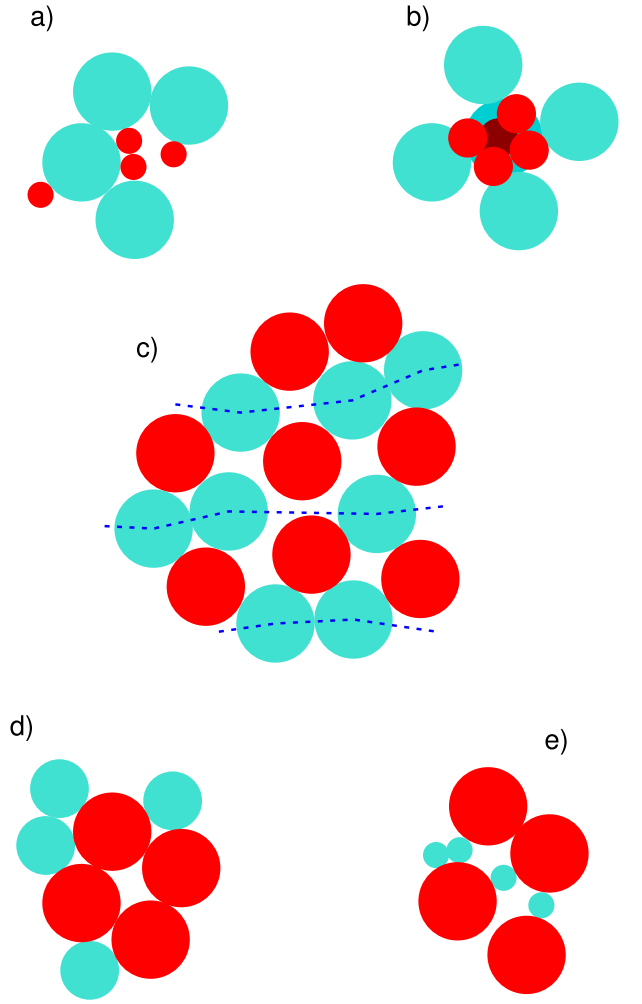

FIG. 8. Possible snapshots of SJD aggregates (or "contact configurations") compatible with the previous cavity function results, for several geometries: (a) $\sigma_B = \sigma_A/3$; (b) $\sigma_B = \sigma_A/2$; (c) $\sigma_B = \sigma_A$; (d) $\sigma_B = (4/3)\sigma_A$; and (e) $\sigma_B = 3\sigma_A$. Further explanations are given in the text.

and protected by the corresponding HS "outside shell," that AB-contacts among different molecules become impossible, while the number of the BB-ones increases as the size of the aggregates grows. Fig. 8(b) displays such an arrangement (here, the third dimension would be essential).

Fig. 5 takes into account the homonuclear case with $\sigma_B = \sigma_A$ ($\mathcal{R}_{\rm SHS} = 0.50$). In the upper panel with $\tau = 0.2$ one observes that $\overline{y}_{AB} \approx \overline{y}_{AA} > \overline{y}_{BB}$, i.e., the numbers of AB- and AA-contacts are practically equivalent for $\rho^* \lesssim 0.3$, while the BB-ones are less frequent. Decreasing the temperature—see the lower panel with $\tau = 0.02$—leads to a further decrease of BB-contacts (apart a small peak of $\overline{y}_{BB}$ not much visible in Fig. 5, at very low densities near $\rho^* = 0$, where $\overline{y}_{BB} \approx \overline{y}_{AB}$), while the AB-contacts become predominant. The snapshot of Fig. 8(c) illustrates the arrangement at low temperature: here we have drawn $\mathcal{N} = 8$ dumbbells, with $m_{AA} = 3$, $m_{AB} = 10$, $m_{BB} = 1$. The dashed lines identify possible lamellar planes.

Fig. 6 corresponds to $\sigma_B = \frac{4}{3}\sigma_A$ ($\mathcal{R}_{\rm SHS} = 0.57$): now the attractive B-part of the dumbbell is slightly predominant. In the upper panel with $\tau = 0.2$ one sees $\overline{y}_{BB} > \overline{y}_{AB} > \overline{y}_{AA}$ at very low densities. Then, the AB-contacts become numerous for $\rho^* \gtrsim 0.05$. In the lower panel, the behavior is similar, but the peak of $\overline{y}_{BB}$ is remarkably strong at low densities. Fig. 8(d) reports a possible snapshot corresponding to such a BB-maximum at low density/low temperature: an aggregate of $\mathcal{N} = 4$ dumbbells with contact numbers $m_{AA} = 1$, $m_{AB} = 3$, $m_{BB} = 4$.

In Fig. 7, referring to $\sigma_B = 3\sigma_A$ ($\mathcal{R}_{\rm SHS} = 0.75$), for both temperatures the AB-contacts are the most important at low densities, while the AA-ones are the most suppressed. As in Fig. 6, there is a prevalence of AB-contacts at moderate and high densities. Fig. 8(e) shows a configuration at high density/low temperature, with $m_{AA} = 1$, $m_{AB} = 3$, $m_{BB} = 1$.

In conclusion, despite some differences among the models, our numerical results appear to be qualitatively compatible with the structural scenario depicted in Refs. 7

and 40–42. Our naïve drawings also suggest the following remark: it is plausible that when the Janus dumbbells have different diameters, i.e., for $\sigma_B \neq \sigma_A$, their overall, more or less pronounced, *cone-like* shape and the A–A attraction are the driving factors, which *always* lead to the formation of micelles.[40] For $\sigma_B \leq \sigma_A$ these spontaneous aggregates have a B-core and an A-outside, whereas for $\sigma_B \geq \sigma_A$ one has A-core and B-outside (see, for instance, Fig. 14 of Ref. 7, although we employ different colors). Spherical micelles are observed even for $\sigma_B = \sigma_A$, although the dumbbell geometry allows for their formation only at very low densities and temperatures. Overall, the system would be regarded as a "simple fluid," built up by "super-particles" identified with the micellar clusters. Since the interaction between these super-particles is characterized by the species involved in the "outside shell," the phase behavior found in the MC simulations can be understood in a very simple way. For $\sigma_B \leq \sigma_A$ the super-particles interact as HS, so that no liquid-vapor phase transition is possible. On the contrary, for $\sigma_B \geq \sigma_A$ the super-particles behave essentially as SW or SHS "simple-particles"; due to the presence of an attractive term in the potential, a liquid-vapor phase transition is now allowed. Probably, for $\sigma_B \geq \sigma_A$ the clustering exists at the beginning but would then become hidden very fast, since the divergence of $S_{BB}(k \to 0)$ overcomes the presence of a low-k prepeak, which disappears while the clusters merge.

Finally, more insight may be obtained through a systematic cluster analysis that makes it possible to identify typical aggregate shapes in terms of three cluster order parameters, as applied by Avvisati *et al.*[8] to the self-assembly of patchy colloidal dumbbells. In their dumbbell model the A and B spheres were not tangential, but intersecting each other with center-center separation $\ell < (\sigma_A + \sigma_B)/2$, while the SW interaction range was again half the diameter of the attractive monomer. The authors showed that by varying the size ratio σ_B/σ_A, the sphere separation ℓ, as well as the volume fraction η, one can obtain the formation of a large variety of structures: spherical micelles, elongated micelles, hollow vesicles, double-layers, liquid-like droplets, and even faceted polyhedra.

VI. CONCLUSIONS

In this paper we have developed the fully analytic solution of Wertheim's two-density integral equations for a fluid of heteronuclear sticky Janus dumbbells within the associative Percus-Yevick approximation. Our analysis extends and completes a previous theoretical study by Wu and Chiew, only limited to dumbbells made up of equal-size monomers. Explicit expressions for all the parameters intervening in the Baxter factor correlation functions have been given, which would greatly simplify the comparison of specific cases with simulation data. Our approach provides results for the contact values of cavity functions that reasonably agree with the overall phase scenario emerging from MC simulations. In a preliminary comparison with simulation data by Munaò *et al.*[7] for SW-Janus-dumbbells, we have checked that in the hard-dumbbell limit our sticky-Janus-dumbbell predictions quantitatively agree with the MC results from the former model. On the other hand, upon progressively switching on the attractive interactions, the differences between SW-JD and SJD models seem to increase. In this respect, we anticipate that further extensive Monte Carlo simulations are currently underway, where the sticky potential is replaced by one with a "narrow" square-well attractive corona. We defer to a forthcoming paper the detailed analysis of the structural differences between these two fluid models, together with the elucidation of the conditions allowing for a meaningful comparison between their structures.

ACKNOWLEDGMENTS

We thank Achille Giacometti (University Ca' Foscari, Venezia) for suggesting the subject of the present research. We are also grateful to Riccardo Fantoni for help with Wolfram Mathematica software. One of us (D.G.) has carried out part of this work as a participant to a PRIN-MIUR 2010-2011 project.

APPENDIX A: DETAILS OF ANALYTIC COMPUTATION

Replacing $h_{ij}^{\alpha\beta}$ with $g_{ij}^{\alpha\beta} - \delta_{i0}\delta_{j0}$ in Eq. (24) gives

$$r g_{ij}^{\alpha\beta}(|r|) + \left[q_{ij}^{\alpha\beta}(r)\right]' = \left(a_i^\alpha r + b_i^\alpha\right)\delta_{j0} + \Gamma_{ij}^{\alpha\beta}(r), \quad \text{(A1)}$$

with

$$\begin{cases} a_i^\alpha = \delta_{i0} - 2\pi \sum_\gamma \sum_k \rho_{k0}^\gamma \int_{L_{\alpha\gamma}}^{\sigma_{\alpha\gamma}} dz\, q_{ik}^{\alpha\gamma}(z), \\ b_i^\alpha = 2\pi \sum_\gamma \sum_k \rho_{k0}^\gamma \int_{L_{\alpha\gamma}}^{\sigma_{\alpha\gamma}} dz\, q_{ik}^{\alpha\gamma}(z)\, z, \end{cases} \quad \text{(A2)}$$

and

$$\Gamma_{ij}^{\alpha\beta}(r) = 2\pi \sum_\gamma \sum_{k,\ell} \rho_{k\ell}^\gamma \int_{L_{\alpha\gamma}}^{\sigma_{\alpha\gamma}} dz\, q_{ik}^{\alpha\gamma}(z) \times g_{\ell j}^{\gamma\beta}(|r-z|)\,(r-z)\,. \quad \text{(A3)}$$

Let us decompose $g_{ij}^{\alpha\beta}$ into regular (*reg*) and singular (*sg*) parts, i.e., $g_{ij}^{\alpha\beta}(|r|) = g_{ij}^{\alpha\beta,\mathrm{reg}}(|r|) + K_{ij}^{\alpha\beta}\,\sigma_{\alpha\beta}\delta(|r| - \sigma_{\alpha\beta})$, taking also into account the identity $\delta(|x| - x_0) = \delta(x - x_0) + \delta(x + x_0)$. Then

(i) the l.h.s. of Eq. (A1) becomes

$$r g_{ij}^{\alpha\beta,\mathrm{reg}}(|r|) + K_{ij}^{\alpha\beta}\sigma_{\alpha\beta} \times \left[\delta(r - \sigma_{\alpha\beta}) + \delta(r + \sigma_{\alpha\beta})\right] + \left[q_{ij}^{\alpha\beta}(r)\right]',$$

where $\delta(r + \sigma_{\alpha\beta})$ can immediately be neglected since it would "act" at $r = -\sigma_{\alpha\beta}$, while r must satisfy the constraint $r \geq L_{\alpha\beta} > -\sigma_{\alpha\beta}$.

(ii) On the r.h.s. of Eq. (A1), $\Gamma_{ij}^{\alpha\beta}(r)$ splits into $\Gamma_{ij}^{\alpha\beta,\mathrm{reg}}(r) + \Gamma_{ij}^{\alpha\beta,\mathrm{sg}}(r)$. The first contribution $\Gamma_{ij}^{\alpha\beta,\mathrm{reg}}(r)$ is given by Eq. (A3) with $g_{\ell j}^{\gamma\beta}$ replaced by $g_{ij}^{\gamma\beta,\mathrm{reg}}$. Since the integration range is $L_{\alpha\gamma} \leq z \leq \sigma_{\alpha\gamma}$, it can be shown that one has $|r - z| < \sigma_{\gamma\beta}$ when $L_{\alpha\beta} < r < \sigma_{\alpha\beta}$. Due to the hard-core conditions Eq. (16), this implies that $g_{\ell j}^{\gamma\beta}(|r - z|) = 0$ and

$$\Gamma_{ij}^{\alpha\beta,\mathrm{reg}}(r) = 0 \qquad \text{for } L_{\alpha\beta} < r < \sigma_{\alpha\beta}. \quad \text{(A4)}$$

Furthermore, the definition of $\Gamma_{ij}^{\alpha\beta,\mathrm{reg}}(r)$ involves integration, which "smoothes" the possible discontinuities of the integrand functions. Thus, the $\Gamma_{ij}^{\alpha\beta,\mathrm{reg}}(r)$'s are continuous functions, and one finds at contact: $\Gamma_{ij}^{\alpha\beta,\mathrm{reg}}(\sigma_{\alpha\beta}^-) = \Gamma_{ij}^{\alpha\beta,\mathrm{reg}}(\sigma_{\alpha\beta}^+) = 0$.

To evaluate the second term $\Gamma_{ij}^{\alpha\beta,\mathrm{sg}}(r)$, we have exploited the identity $\delta(|z-r|-\sigma_{\gamma\beta}) = \delta(z-z_-)+\delta(z-z_+)$ with $z_\pm = r \pm \sigma_{\gamma\beta}$, as well as the relation

$$\begin{aligned}\int_{L_{\alpha\gamma}}^{\sigma_{\alpha\gamma}} dz\; q_{ik}^{\alpha\gamma}(z)\,(r-z)\;\;\delta(z-z_\pm) &= \int_{L_{\alpha\gamma}}^{\sigma_{\alpha\gamma}} dz\;\;\left[\pm\sigma_{\gamma\beta}\, q_{ik}^{\alpha\gamma}(z_\pm)\right]\;\delta(z-z_\pm)\\ &= \pm\sigma_{\gamma\beta}\, q_{ik}^{\alpha\gamma}(z_\pm)\int_{L_{\alpha\gamma}}^{\sigma_{\alpha\gamma}} dz\;\;\delta(z-z_\pm).\end{aligned}$$

The expression for $\Gamma_{ij}^{\alpha\beta,\mathrm{sg}}(r)$ then includes the factor

$$\begin{aligned}&q_{ik}^{\alpha\gamma}(z_+)\int_{L_{\alpha\gamma}}^{\sigma_{\alpha\gamma}} dz\;\;\delta(z-z_+)\\ &\quad - q_{ik}^{\alpha\gamma}(z_-)\int_{L_{\alpha\gamma}}^{\sigma_{\alpha\gamma}} dz\;\;\delta(z-z_-).\end{aligned}\tag{A5}$$

Now, from the definition of δ-function it follows that

$$\begin{aligned}\int_a^b dx\;\delta(x-x_0) &= \Theta(x_0-a)\Theta(b-x_0)\\ &= \begin{cases}1 & \text{if}\quad a<x_0<b\\ 0 & \text{otherwise}\end{cases},\end{aligned}\tag{A6}$$

where Θ is the Heaviside function, with $\Theta(x>0)=1$ and $\Theta(x<0)=1$. We thus obtain

$$\begin{aligned}\Gamma_{ij}^{\alpha\beta,\mathrm{sg}}(r) = 2\pi\sum_\gamma\sum_{k,\ell}\rho_{k\ell}^\gamma K_{ij}^{\gamma\beta}\sigma_{\gamma\beta}^2 &\times\left[\, q_{ik}^{\alpha\gamma}(r-\sigma_{\gamma\beta})\Theta(r-\sigma_{\alpha\beta})\Theta(\sigma_{\alpha\beta}+\sigma_\gamma-r)\right.\\ &\left.- q_{ik}^{\alpha\gamma}(r+\sigma_{\gamma\beta})\Theta(r-L_{\alpha\beta}+\sigma_\gamma)\Theta(L_{\alpha\beta}-r)\right]\end{aligned}$$

and, since $r > L_{\alpha\beta}$, the expression reduces to

$$\begin{aligned}\Gamma_{ij}^{\alpha\beta,\mathrm{sg}}(r) = \Theta(r-\sigma_{\alpha\beta})\,2\pi\sum_\gamma\sum_{k,\ell}\rho_{k\ell}^\gamma K_{ij}^{\gamma\beta}\sigma_{\gamma\beta}^2 &\times q_{ik}^{\alpha\gamma}(r-\sigma_{\gamma\beta})\Theta(\sigma_{\alpha\beta}+\sigma_\gamma-r).\end{aligned}\tag{A7}$$

As a result, we also get

$$\Gamma_{ij}^{\alpha\beta,\mathrm{sg}}(r) = 0 \qquad \text{for } L_{\alpha\beta} < r < \sigma_{\alpha\beta}.$$

In conclusion, in the interval $(L_{\alpha\beta},\sigma_{\alpha\beta})$ Eq. (A1) becomes

$$\left[q_{ij}^{\alpha\beta}(r)\right]' = \left(a_i^\alpha r + b_i^\alpha\right)\,\delta_{j0} - K_{ij}^{\alpha\beta}\sigma_{\alpha\beta}\,\delta(r-\sigma_{\alpha\beta}).\tag{A8}$$

Integrating, and taking into account Eq. (23), we obtain

$$q_{ij}^{\alpha\beta}(r) = \begin{cases}\left[\frac{1}{2}a_i^\alpha\left(r^2-\sigma_{\alpha\beta}^2\right)+b_i^\alpha\left(r-\sigma_{\alpha\beta}\right)\right]\,\delta_{j0}+K_{ij}^{\alpha\beta}\sigma_{\alpha\beta}^2 & L_{\alpha\beta}\le r\le\sigma_{\alpha\beta}\\ 0 & \text{elsewhere}\end{cases},\tag{A9}$$

where the set of parameters $\left\{a_i^\alpha, b_i^\alpha, K_{ij}^{\alpha\beta}\right\}$ is yet to be determined.

Using this expression for $q_{ij}^{\alpha\beta}(r)$ in Eqs. (A2) leads to a set of equations for the parameters

$$\begin{cases}\left(1-\xi_3-3\xi_2\sigma_\alpha\right)a_i^\alpha - 6\xi_2 b_i^\alpha = \delta_{i0} - X_i^\alpha,\\ \frac{3}{2}\xi_2\sigma_\alpha^2\, a_i^\alpha + \left(1-\xi_3+3\xi_2\sigma_\alpha\right)b_i^\alpha = \frac{1}{2}X_i^\alpha\sigma_\alpha,\end{cases}\tag{A10}$$

where $\xi_m = \frac{\pi}{6}\sum_\gamma \rho_\gamma\sigma_\gamma^m$ and $X_i^\alpha = 2\pi\sum_\gamma\sigma_\gamma\sigma_{\alpha\gamma}^2\sum_k\rho_{k0}^\gamma K_{ik}^{\alpha\gamma}$. The solution to this system, reported in Eqs. (30)-(33), gives $\left\{a_i^\alpha, b_i^\alpha\right\}$ as functions of $\left\{K_{ij}^{\alpha\beta}\right\}$, which thus remain the last parameters to be determined.

APPENDIX B: WORKING ON PARAMETERS

Splitting both $g_{ij}^{\alpha\beta}$ and $\left[q_{ij}^{\alpha\beta}\right]'$ into a regular and a singular part, the two delta terms cancel each other, so that Eq. (A1) becomes

$$\begin{aligned}r g_{ij}^{\alpha\beta,\mathrm{reg}}(|r|) + \left[q_{ij}^{\alpha\beta,\mathrm{reg}}(r)\right]' &= \left(a_i^\alpha r + b_i^\alpha\right)\delta_{j0} + \Gamma_{ij}^{\alpha\beta,\mathrm{reg}}(r) + \Gamma_{ij}^{\alpha\beta,\mathrm{sg}}(r).\end{aligned}\tag{B1}$$

Let us study it at $r=\sigma_{\alpha\beta}^+$. Here, one has $g_{ij}^{\alpha\beta,\mathrm{reg}}(\sigma_{\alpha\beta}^+) = y_{ij}^{\alpha\beta}(\sigma_{\alpha\beta})$, $\left[q_{ij}^{\alpha\beta,\mathrm{reg}}\right]'(\sigma_{\alpha\beta}^+) = \Gamma_{ij}^{\alpha\beta,\mathrm{reg}}(\sigma_{\alpha\beta}^+) = 0$. Using Eq. (A7) we then arrive at the following expressions for the cavity correlation functions at contact

$$\begin{aligned}\sigma_{\alpha\beta}\, y_{ij}^{\alpha\beta}(\sigma_{\alpha\beta}) &= \left(a_i^\alpha\sigma_{\alpha\beta}+b_i^\alpha\right)\delta_{j0} + 2\pi\sum_\gamma\sum_{k,\ell} q_{ik}^{\alpha\gamma}(L_{\alpha\gamma}^+)\\ &\quad\times\rho_{k\ell}^\gamma\, q_{\ell j}^{\alpha\gamma}(\sigma_{\alpha\gamma}^-),\end{aligned}\tag{B2}$$

where $q_{\ell j}^{\alpha\gamma}(\sigma_{\alpha\gamma}^-) = K_{\ell j}^{\gamma\beta}\sigma_{\gamma\beta}^2$. From Eqs. (30) and (31) we get

$$a_i^\alpha\sigma_{\alpha\beta}+b_i^\alpha = \left(\frac{1}{\Delta}\sigma_{\alpha\beta}+\frac{3\xi_2}{2\Delta^2}\sigma_\alpha\sigma_\beta\right)\delta_{i0} - \frac{X_i^\alpha}{2\Delta}\sigma_\beta,\tag{B3}$$

as well as

$$q_{ik}^{\alpha\gamma}(L_{\alpha\gamma}^{+}) = -\left(\frac{1}{2}a_i^{\alpha}\sigma_{\alpha} + b_i^{\alpha}\right)\sigma_{\gamma}\,\delta_{k0} + K_{ik}^{\alpha\gamma}\sigma_{\alpha\gamma}^{2}$$
$$= -\frac{1}{2\Delta}\sigma_{\alpha}\sigma_{\gamma}\,\delta_{i0}\delta_{k0} + K_{ik}^{\alpha\gamma}\sigma_{\alpha\gamma}^{2}. \quad \text{(B4)}$$

The condition $q_{ij}^{\alpha\beta}(L_{\alpha\beta}) = q_{ji}^{\beta\alpha}(L_{\beta\alpha})$ implies that

$$K_{ij}^{\alpha\beta} = K_{ji}^{\beta\alpha}, \quad \text{(B5)}$$

and this allows us to arrive at the final result given by Eqs. (62) and (63).

[1]A. Walther and A. H. E. Müller, Chem. Rev. **113**, 5194 (2013).
[2]Z. He and I. Kretzschmar, Langmuir **29**, 15755 (2013).
[3]J. Zhang, E. Luijten, and S. Granick, Annu. Rev. Phys. Chem. **66**, 581 (2015).
[4]G. Munaò, D. Costa, A. Giacometti, C. Caccamo, and F. Sciortino, Phys. Chem. Chem. Phys. **15**, 20590 (2013).
[5]G. Munaò, P. O'Toole, T. S. Hudson, D. Costa, C. Caccamo, A. Giacometti, and F. Sciortino, Soft Matter **10**, 5269 (2014).
[6]G. Munaò, F. Gámez, D. Costa, C. Caccamo, F. Sciortino, and A. Giacometti, J. Chem. Phys. **142**, 224904 (2015).
[7]G. Munaò, P. O'Toole, T. S. Hudson, D. Costa, C. Caccamo, F. Sciortino, and A. Giacometti, J. Phys.: Condens. Matter **27**, 234101 (2015).
[8]G. Avvisati, T. Vissers, and M. Dijkstra, J. Chem. Phys. **142**, 084905 (2015).
[9]R. J. Baxter, J. Chem. Phys. **49**, 2270 (1968).
[10]D. Chandler and H. C. Andersen, J. Chem. Phys. **57**, 1930 (1972).
[11]M. S. Wertheim, J. Stat. Phys. **35**, 19 (1984).
[12]M. S. Wertheim, J. Stat. Phys. **35**, 35 (1984).
[13]M. S. Wertheim, J. Stat. Phys. **42**, 459 (1986).
[14]M. S. Wertheim, J. Stat. Phys. **42**, 477 (1986).
[15]M. S. Wertheim, J. Chem. Phys. **85**, 2929 (1986).
[16]Y. V. Kalyuzhnyi and G. Stell, Mol. Phys. **78**, 1247 (1993).
[17]Y. V. Kalyuzhnyi, I. A. Protsykevytch, and M. F. Holovko, Chem. Phys. Lett. **215**, 1 (1993).
[18]A. O. Weist and E. D. Glandt, J. Chem. Phys. **95**, 8365 (1991).
[19]A. O. Weist and E. D. Glandt, J. Chem. Phys. **97**, 4316 (1992).
[20]N. Wu, S. S. Feng, and Y. C. Chiew, J. Chem. Phys. **117**, 4462 (2002).
[21]Y. V. Kalyuzhnyi, L. Blum, J. Reščič, and G. Stell, J. Chem. Phys. **113**, 1135 (2000).
[22]M. F. Holovko and Y. V. Kalyuzhnyi, Mol. Phys. **73**, 1145 (1991).
[23]Y. V. Kalyuzhnyi and V. Vlachy, Chem. Phys. Lett. **215**, 518 (1993).
[24]Y. V. Kalyuzhnyi, V. Vlachy, M. F. Holovko, and G. Stell, J. Chem. Phys. **102**, 5770 (1995).
[25]I. A. Protsykevytch, Chem. Phys. Lett. **252**, 431 (1996).
[26]Y. V. Kalyuzhnyi, L. Blum, M. F. Holovko, and I. A. Protsykevytch, Physica A **236**, 85 (1997).
[27]N. von Solms and Y. C. Chiew, J. Chem. Phys. **113**, 6316 (2000).
[28]J. Chang and S. I. Sandler, J. Chem. Phys. **102**, 437 (1995).
[29]J. Chang and S. I. Sandler, J. Chem. Phys. **103**, 3196 (1995).
[30]N. Wu, S. S. Feng, and Y. C. Chiew, J. Chem. Phys. **118**, 10794 (2003).
[31]N. Wu and Y. C. Chiew, Phys. Rev. E **81**, 041809 (2010).
[32]L. Blum, M. F. Holovko, and I. A. Protsykevytch, J. Stat. Phys. **84**, 191 (1996).
[33]I. A. Protsykevytch, Y. V. Kalyuzhnyi, M. F. Holovko, and L. Blum, J. Mol. Liq. **73-74**, 1 (1997).
[34]Y. V. Kalyuzhnyi, Condens. Matter Phys. **11**, 71 (1997).
[35]Y. V. Kalyuzhnyi and P. T. Cummings, in *Equations of State for Fluids and Fluid Mixtures, Part I*, edited by J. V. Sengers, R. F. Kayser, C. J. Peters, and H. J. White, Jr. (Elsevier, Amsterdam, 2000), Chap. 6.
[36]J. P. Hansen and I. R. McDonald, *Theory of Simple Liquids*, 3rd ed. (Elsevier, Amsterdam, 2006).
[37]N. Wu and Y. C. Chiew, J. Chem. Phys. **115**, 6641 (2001).
[38]R. O. Watts, D. Henderson, and R. J. Baxter, in *Advances in Chemical Physics,* Vol. 21, edited by J. O. Hirschfelder and D. Henderson (Wiley, Hoboken NJ, 1971), p. 421.
[39]J. W. Perram, Mol. Phys. **30**, 1505 (1975).
[40]D. J. Kraft, R. Ni, F. Smallenburg, M. Hermes, K. Yoon, D. A. Weitz, A. van Blaaderen, J. Groenewold, M. Dijkstra, and W. K. Kegel, Proc. Natl. Acad. Sci. U. S. A. **109**, 10787 (2012).
[41]L. Hong, A. Cacciuto, E. Luijten, and S. Granick, Nano Lett. **6**, 2510 (2006).
[42]L. Hong, A. Cacciuto, E. Luijten, and S. Granick, Langmuir **24**, 621 (2008).
[43]J. A. Barker and D. Henderson, Rev. Mod. Phys. **48**, 587 (1976).